Helsinki University of Technology Publications in Engineering Physics
Teknillisen korkeakoulun teknillisen fysiikan julkaisuja
Espoo 2004 TKK-F-A831

PERFORMANCE LIMITATIONS AND IMPROVEMENTS OF SMALL-SCALE FREE-BREATHING POLYMER ELECTROLYTE MEMBRANE FUEL CELLS

Tero Hottinen

Dissertation for the degree of Doctor of Science in Technology to be presented with due permission of the Department of Engineering Physics and Mathematics, Helsinki University of Technology for public examination and debate in Auditorium F1 at Helsinki University of Technology (Espoo, Finland) on the 1st of October, 2004, at 12 o'clock noon.

Helsinki University of Technology
Department of Engineering Physics and Mathematics
Laboratory of Advanced Energy Systems

Distribution:
Helsinki University of Technology
Laboratory of Advanced Energy Systems
P.O. Box 2200
FIN-02015 HUT
Finland
Tel. +358-9-451-3198
Fax +358-9-451-3195
E-mail: tero.hottinen@hut.fi

ISBN 951-22-7254-7
ISBN 951-22-7255-5 (pdf)

ISSN 1456-3320
ISSN 1459-7268 (pdf)

Electronic version available at: http://lib.hut.fi/Diss/2004/isbn9512272555/

Otamedia Oy

Espoo 2004

Preface

The work presented in this thesis was carried out at the Laboratory of Advanced Energy Systems in Helsinki University of Technology. National Technology Agency of Finland (TEKES), Fortum Foundation, and Graduate School for Energy Technology are gratefully acknowledged for funding the work. In addition, SGL Technologies GmbH and Labgas Instrument Co are acknowledged for providing part of the materials used in the measurements of this thesis.

I would like to thank Prof. Peter Lund for giving me the possibility to work in the laboratory. It has been a great opportunity to be able to make a dissertation under his supervision on such an interesting subject. I am deeply indebted for the core members, past and present, of the laboratory's fuel cell group: Dr. Matti Noponen, Dr. Tuomas Mennola, Mr. Mikko Mikkola, and Mr. Olli Himanen. Without your contribution this thesis would have been too tremendous a task to do. In addition, I would like to thank Matti and Olli, and naturally Mr. Klaus Mäki-Petäys, for all of those on-topic and especially off-topic discussions during the years spent in the same office.

Finally, I would like to express my gratitude to my wife Hanna-Leena and my parents Raimo and Kirsi for the never-ending support. In addition, I would like to thank my family and friends for understanding the lack of time for them; Finalizing a dissertation, having a pregnant wife, and building a house at the same time can be rather hectic every now and then.

Espoo, September 2004

Tero Hottinen

Abstract

Fuel cell is an electrochemical device that converts the chemical energy of fuel directly into electricity and heat without combustion with flame. The range of potential applications is from small-scale portable electronics to transportation and large-scale power production. An interesting approach for small-scale applications are free-breathing fuel cells, i.e. cells that take the oxygen needed in the reactions passively from ambient air. This thesis concentrates on performance limitations caused by the use of passive air supply in small-scale polymer electrolyte membrane fuel cells (PEMFCs) and aims to find solutions for these limitations.

A conventional free-breathing PEMFC with vertical cathode channels was studied with a current distribution measurement system at different cell temperatures and ambient conditions. In addition, different overpotential distributions were determined with a flow pulse method, and a mass transport model for the cathode side of the cell was developed. The results showed that with this kind of a cell design, the main limiting factor is the mass transfer in the cathode channels. In order to enhance the air flow and thus to improve mass transfer, there should be a high temperature difference between the cell and ambient air. High cell temperature would also decrease liquid water saturation, which would be beneficial since it causes additional mass transfer limitations.

The mass transfer limitations can also be reduced with wider channels. However, wide channels require a rigid gas diffusion backing in order to offer adequate support for the membrane. A potential mechanically rigid material, titanium sinter, was introduced in the thesis. Another possible solution for reduction of mass transfer limitations is a so-called planar free-breathing cell design in which there is more effective area for cathode side mass transfer than in traditional design. This cell design was introduced and its performance with different cathode structures was studied in the thesis. The results with certain cathode structure showed very high power densities for a free-breathing fuel cell.

According to the results achieved in this thesis, it seems that free-breathing PEMFCs are a very potential power source for small-scale applications such as consumer electronics. As an outcome of this thesis the performance limitations of free-breathing PEMFCs are better known, and possible solutions for them are introduced.

Table of Contents

List of Publications

This thesis is an introduction to the following publications:

I M. Noponen, T. Mennola, M. Mikkola, T. Hottinen, P. Lund, '*Measurement of current distribution in a free-breathing PEMFC*', J. Power Sources 106 (2002) 304-312.

II T. Hottinen, M. Noponen, T. Mennola, O. Himanen, M. Mikkola, P. Lund, '*Effect of ambient conditions on performance and current distribution of a polymer electrolyte membrane fuel cell*', J. Appl. Electrochem. 33 (2003) 265-271.

III M. Noponen, T. Hottinen, T. Mennola, M. Mikkola, P. Lund, '*Determination of mass diffusion overpotential distribution with flow pulse method from current distribution measurements in a PEMFC*', J. Appl. Electrochem. 32 (2002) 1081-1089.

IV T. Mennola, M. Noponen, M. Aronniemi, T. Hottinen, M. Mikkola, O. Himanen, P. Lund, '*Mass transport in the cathode of a free-breathing polymer electrolyte membrane fuel cell*', J. Appl. Electrochem. 33 (2003) 979-987.

V T. Hottinen, M. Mikkola, T. Mennola, P. Lund, '*Titanium sinter as gas diffusion backing in PEMFC*', J. Power Sources 118 (2003) 183-188.

VI T. Hottinen, M. Mikkola, P. Lund, '*Evaluation of planar free-breathing polymer electrolyte membrane fuel cell design*', J. Power Sources 129 (2004) 68-72.

VII T. Hottinen, O. Himanen, P. Lund, '*Effect of cathode structure on planar free-breathing PEMFC*', J. Power Sources, in press.

Contents of the Publications and Author's Contribution

I A measurement system for the mapping of current distribution in a free-breathing PEMFC was introduced. Measurements were conducted in different cell temperatures and it was concluded that enhanced convection caused by elevated temperatures yield more homogeneous current distribution profiles. In addition, a model was implemented in order to discuss the effect of non-segmented gas diffusion backing.

The author assisted in the construction of the measurement system and had a minor role in the writing process.

II The effect of ambient conditions on the performance and current distribution of a free-breathing PEMFC was studied. The cell was placed into a climate chamber, in which temperature and relative humidity of air can be controlled. It was concluded that a temperature gradient is needed between the cell and ambient air in order to enhance the convection. Enhanced convection offers more oxygen to the active area and especially removes excess water from the cell preventing flooding.

The author designed the experiments and contributed in conducting them. The author was mainly responsible for the analysis of the results and was the main author of the manuscript.

III A flow pulse method was developed in order to be able to estimate the magnitude of different overpotential distributions. Strong air pulse was fed to the cathode channels. Overpotential distributions were estimated from the difference between flow pulse measurements and normal operation.

The author assisted in the measurements, and participated actively in the results analysis and the writing process.

IV A model for the cathode of a free-breathing PEMFC was developed. Measured current distributions were used as boundary condition for the model. The purpose of the model was to predict the molar fractions of oxygen and water vapor, and the flow velocity in the cathode channels. It was concluded that diffusion is a minor mass transport effect compared to temperature driven convection. In addition, the model implied that this type of fuel cell is vulnerable for liquid water saturation.

The author conducted part of the measurements and participated in the writing of the article.

V The applicability of titanium sinter material as a gas diffusion backing was evaluated. The major problem was found to be the contact resistance between Ti sinter and MEA. Platinum coating reduced the contact resistance, but still the sinter material operated somewhat weaker than traditional carbon paper gas diffusion backing.

The author was mainly responsible for designing the experiments and also conducted them. The author was also mainly responsible for the analysis of the results and was the main author of the manuscript.

VI The concept of a planar free-breathing PEMFC design was introduced. The polarization, long-term, and current transient measurements showed that this kind of a free-breathing fuel cell may have potential in small-scale applications such as portable electronics.

The author designed the cell structure in close cooperation with the co-authors. The author was mainly responsible for the rest of the article.

VII The effect of cathode structure on the performance of a planar free-breathing PEMFC was studied by varying the current collector plate structure and cathode gas diffusion backing. With thick gas diffusion backings the effect of current collector was minor, whereas with thin gas diffusion backing the effect was significant. The results showed very high power densities for free-breathing fuel cell.

The author was mainly responsible for all parts of the article.

1 Introduction

1.1 General

Environmental problems due to energy production and transportation sector have attracted increasing interest throughout the last decades. The global energy consumption has increased over 14% during last decade [1]. The population of the Earth is growing and due to simultaneous economic growth it seems more than likely that the total energy consumption will continue to increase furthermore. The acute need for cleaner and more efficient technologies has been one of the main accelerators for the development of the fuel cell technology.

Fuel cell is an electrochemical device that converts the energy of fuel directly into electricity and heat without combustion with flame. If hydrogen is used as a fuel, the only reaction product is pure water and with low-temperature fuel cells no direct harmful emissions occur. Even though the interest towards fuel cells has not been that significant until last decade, the fuel cell itself is an old invention. The fuel cell reaction was first observed in 1838 by Prof. Christian Friedrich Schönbein, and the actual fuel cell was invented in 1842 by Sir William Robert Grove, who is regarded as the father of the fuel cell [2].

The first major leap in the development of fuel cells took place in the late 1950's when NASA started their fuel cell program. The high gravimetric energy density of the fuel cell technology was interesting for space applications in which the cost was not a critical issue. The first fuel cell used in space application was in 1960's in Gemini missions, in which the fuel cell was used to provide electricity and drinking water [3, 4].

Starting from the late 1960's there have been several projects aiming to bring down the cost of the fuel cell in order to be competitive also in terrestrial applications. Nowadays, after several technological breakthroughs, such as thin-film electrodes and reduced corrosion, the fuel cells are on the threshold of market penetration.

There are several different fuel cell types named after their electrolyte. This thesis concentrates on the polymer electrolyte membrane fuel cell (PEMFC) also known as proton exchange membrane fuel cell, solid polymer fuel cell (SPFC), and polymer electrolyte fuel cell (PEFC). The other main fuel cell types are solid oxide fuel cell (SOFC), molten carbonate fuel cell (MCFC), alkaline fuel cell (AFC), and phosphoric acid fuel cell (PAFC) which was the first commercial fuel cell type [4]. There are also fuel cell types that are based on direct oxidation of alcohols, such as direct methanol and direct ethanol fuel cell (DMFC, DEFC), but structurally they are very similar to PEMFC.

The application range considered suitable for fuel cells is very large ranging from large-scale combined heat and power (CHP) production through transportation and auxiliary power unit (APU) applications to portable electronics. One important benefit of fuel cell technology is that the efficiency of a fuel cell is not virtually affected by their size, which is not the case for traditional energy conversion devices based on heat engines. Moreover, the efficiency of a fuel cell is high also on partial loads, which is a significant advantage compared to internal combustion engines.

1.2 Motivation and Objectives

Small-scale applications, such as portable electronics and electric tools, are nowadays mainly powered by batteries. In order to be competitive against batteries, the fuel cell system should have high power density and be as reliable as possible. In small systems, the requirement of high power density may be achieved by minimizing the number of auxiliary control devices. This means that the management of operation, such as feeding of the reactant gases and temperature and water management, should be accomplished with passive methods. The effect of using passive methods on the total volumetric and gravimetric power density of the fuel cell system depends very much on the application. The power density of the fuel cell itself usually decreases with the use of passive methods, but the volume and parasitic power consumption of the fuel cell system are simultaneously decreased as less auxiliary devices are needed.

One interesting approach for powering a small-scale application is free-breathing fuel cells. A free-breathing fuel cell takes the oxygen needed by the fuel cell reaction directly from the surrounding air by natural convection and diffusion eliminating the need of auxiliary air circulation device. The use of passive air supply means that reliable and effective cathode side mass transfer must be achieved by the choice of materials and geometry design.

This thesis concentrates on performance limitations caused by the use of passive air supply in small-scale PEMFCs and aims to find solutions for these limitations. The limitations of a traditional type of free-breathing PEMFC, which has straight air channels open to ambient air, is studied with a current distribution measurement system in different cell temperatures and ambient conditions. The current distribution measurement gives more insight into the losses and their causes than mere polarization curves. In addition, a model for similar cell geometry was developed in order to obtain information on the flow velocities and molar fractions in the cathode channels. Based on the results it is possible to draw conclusions on the causes of the limitations and to find solutions for them.

Possible solutions for the performance limitations observed are offered in the thesis. A novel gas diffusion backing material, mechanically rigid titanium sinter, is introduced and

its potential in replacing traditional materials is evaluated. In addition, based on the mass transfer limitations observed with the traditional free-breathing PEMFC structure, an alternative cell design is introduced. The potential of this so-called planar free-breathing cell design is evaluated, and experiments with different cathode structures are made in order to improve its performance.

1.3 Outline of the Thesis

This thesis starts with an introduction to PEMFCs in Chapter 2. The structure of a PEMFC is explained and the tasks and materials of main functional components are described. The operating principles, including cell reactions, ideal and real performance, and efficiency aspects of the cell are discussed. In addition, an emphasis is given on the local phenomena occurring inside the cell.

The results achieved in this thesis are described in Chapters 3-5. The most important results as well as interconnections between them are highlighted, and the importance and consequences of results are discussed. Chapter 3 is focused on characterization and evaluation of performance limitations of free-breathing PEMFC with straight cathode channels. A review of the results achieved with Ti sinter is given in Chapter 4. Introduction and main results achieved with planar free-breathing cell design are described in Chapter 5.

A summary of the main results and concluding remarks are given in Chapter 6. The publications on which this thesis is based are attached to the end.

2 Polymer Electrolyte Membrane Fuel Cell

2.1 General

Fuel cell is an electrochemical device that converts the chemical energy of fuel directly into electricity and heat. The fuel cell reaction is electrochemical and thus there is no burning with flame as in internal combustion devices. Polymer electrolyte membrane fuel cell (PEMFC) uses hydrogen as fuel and the reaction product is pure water. The half-cell and total reactions of a PEMFC are

Anode: $$H_2 \rightarrow 2H^+ + 2e^- \quad (1)$$

Cathode: $$\frac{1}{2}O_2 + 2H^+ + 2e^- \rightarrow H_2O \quad (2)$$

Total: $$H_2 + \frac{1}{2}O_2 \rightarrow H_2O + electricity + heat \quad (3)$$

A schematic structure of a PEMFC with an illustration of the operation principle is given in Figure 1. The hydrogen fed to the anode is oxidized on the catalyst surface into protons and electrons. Protons are transferred through the electrolyte membrane and electrons via an external circuit to the cathode. The oxygen fed to the cathode is combined with the protons and electrons producing water.

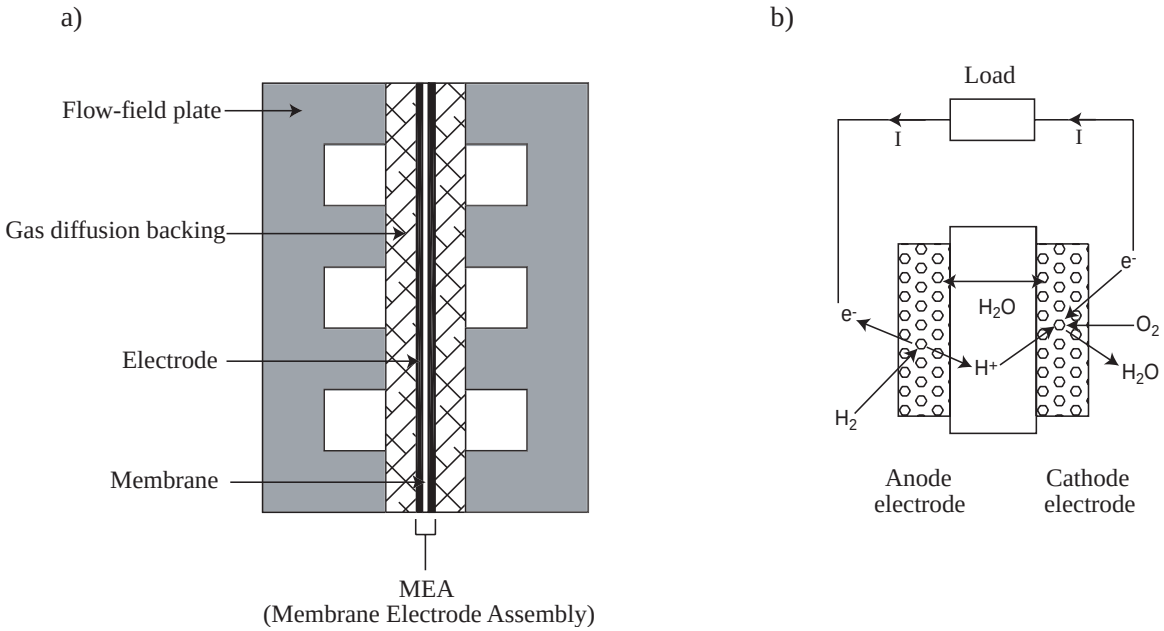

Figure 1. a) Schematic structure and main components of a PEMFC, b) operation principle and material fluxes of a PEMFC.

2.2 Structure

2.2.1 Membrane

The electrolyte of a PEMFC is a solid polymer membrane structure. The membrane operates as a proton conductor enabling the protons released on the anode to travel to the cathode. The membrane has to be an electronic insulator in order not to short-circuit the cell, and it has to be impermeable for reactant gases in order to prevent the direct oxidation of fuel. The membrane material also has to be mechanically and chemically stable.

Most of the PEMFC electrolytes used are based on Nafion® by E.I. du Pont de Nemours and Company. Nafion® consists of a polytetrafluoroethylene (PTFE) backbone on which sulfonic acid groups that enable the charge transfer, i.e. movement of protons, are bonded. Nafion®-like membranes are chemically and mechanically strong, but they have to be hydrated in order to conduct protons. This limits the operating temperature of a typical PEMFC to a range where water is in liquid state.

When the membrane is dry, protons interact strongly with sulfonic acid groups. As the amount of water is increased, the sulfonic acid groups become partly covered with water molecules, and therefore the interaction between protons and sulfonic acid groups weakens enabling the movement of protons from a sulfonic acid to another and thus increasing the conductivity, see e.g. [5-7]. The amount of water inside the membrane depends on the amount of possible humidification of reactant gases and water transport properties of the membrane.

Water transport in the membrane can take place by three different mechanisms. Protons migrating from the anode to the cathode drag water molecules with them. This phenomenon is called the electro-osmotic drag, and its effect has bee studied e.g. in [8-11]. Water transfer by diffusion takes place when there are water concentration gradients across the membrane. Diffusion of water in the membranes has been studied e.g. in [8, 12, 13]. Possible pressure gradients across the membrane cause hydraulic permeation, which has been studied e.g. in [11].

If the membrane is thin, such as the membranes used in this thesis, the amount of product water can be adequate to keep the membrane hydrated. This is important especially for small-scale applications in which it may be desirable to operate the system without external humidification. However, with thin membranes the leakage of reactants is usually also increased, which is an unfavorable property. The typical thickness of membrane varies from tens to a few hundred micrometers.

Several research groups are developing new membrane materials for operating temperatures over 100 °C. These include e.g. different kinds of hybrid and composite membranes, see e.g. [14-16], and phosphoric acid doped PBI membranes, see e.g. [17]. An extensive review on synthesis, chemical, and electrochemical properties of different types of membranes is given in [18].

2.2.2 Electrodes

The fuel cell reactions take place in the electrodes, between which the membrane is located. At the anode hydrogen is oxidized, Equation (1), and at the cathode oxygen is reduced, Equation (2). The reactions require a so-called three phase boundary in order to occur. This means that the catalyst surface has to have access to electronic and protonic conductors, and reactant gas has to be present.

The electrodes are usually made of a porous mixture of carbon black, proton conducting polymer, and platinum particles. Carbon black is a sufficient electronic conductor and enables porous structures that form passages for reactants onto the catalyst surface. Platinum operates as a catalyst ensuring high reaction rates even in the temperature range typical for a PEMFC. Typical platinum loading is in the range of 0.1 – 0.4 mg cm^{-2}. The main problem with platinum catalyst is its intolerance to impurities, especially carbon monoxide, which is usually present in some amounts in reformed hydrogen. In addition, platinum is a rather expensive metal. For these reasons, other types of catalysts such as mixtures of platinum and ruthenium are also being investigated, see e.g. [19-22].

Electrodes are typically sprayed or screen-printed directly in the form of a thin-film electrode onto the membrane. This integrated structure is called the membrane electrode assembly (MEA). The thickness of the electrodes is usually in the scale of micrometers.

2.2.3 Gas Diffusion Backings

Gas diffusion backings are porous structures placed between the MEA and flow-field plates. Gas diffusion backings are made of a porous material because their task is to distribute the reactant gases from the flow-field plates evenly to the electrode. In addition, they have to be good electronic conductors in order to allow the electrons released in the anode electrode to pass to the external circuit and from the external circuit to the cathode electrode. The porosity of the gas diffusion backings also enables the removal of excess product water from the electrode. However, the gas diffusion backing has to have the property of holding back some of the water, since the membrane has to be humidified in order to have proper protonic conduction.

Until recently gas diffusion backings have attracted significantly less attention than the other main components of the fuel cell. However, the gas diffusion backing properties can

have a major influence on the performance of the cell as was shown e.g. in [23]. Some studies have been made trying to explain the performance differences and to find the critical physical properties affecting the performance, see e.g. [24-29]. It was shown by Ihonen et al. [29] that the water management properties of a gas diffusion backing have a major effect on the performance differences in the two-phase region.

The gas diffusion backings are usually made of carbon paper or cloth, and the water removal properties are enhanced with hydrophobic substance such as Teflon®. The typical thickness of a carbon-based gas diffusion backing is a few hundred micrometers. Also other materials, such as metal nets and foams have been studied, see e.g. [30-32]. The rigidity of metallic materials offers some advantageous properties. Compressible carbon materials are compacted under pressure resulting in increased mass transfer limitations, which should not be the case with rigid materials. In addition, with rigid materials the contact between the gas diffusion backing and MEA is more homogeneous even if there were less supporting structure. The minimization of supporting structure may be advantageous especially in small-scale applications, where the weight and size of the cell can be critical. A potential mechanically rigid gas diffusion backing material is introduced in Publication V.

2.2.4 Flow-Field Plates

The flow-field plates are situated next to the gas diffusion backings. The main tasks of the flow-field plate are to provide a passage for the reactants to the active cell area and to remove the product water from diluting the reactant concentration. In addition, flow-field plate typically operates as an electric connection and a gas separator between unit cells of a fuel cell stack. Flow-field plate may also serve as a supporting structure through the gas diffusion backing for flexible MEA.

The channel geometry of the flow-field plate can have a significant effect on the cell performance. There are several aspects that have to be taken into account in the optimization of flow-field geometry. In order to a have homogeneous concentration profile of reactants throughout the cell, the flow resistance of the channels should be minimized and the pressure drop between adjacent channels should be equal. The power consumption of the possible air circulation device is also increased as the pressure drop caused by flow resistance is increased. One possible approach for decreasing the pressure drop is to increase the cross-sectional area of the channels. However, with larger channels the flow velocity is decreased which hinders the liquid water removal from the channels. The cross-sectional area of the channels has some other limitations, too. Increasing the depth of the channel is unfavorable as the thickness of the cell is simultaneously increased. The increase of the channel width may introduce mechanical problems because the ribs between the channels operate as a supporting structure for the MEA. In addition,

with flexible gas diffusion backings the mechanical contact with the MEA in the middle of the channel is weaker, increasing the contact resistance on those parts.

The channel-rib ratio of the flow-field structure is also a critical factor. With narrow ribs the mass transfer in the gas diffusion backing areas beneath the ribs is improved. The areas beneath the ribs may however be compacted, and the loss of porosity brings additional mass transfer limitations. With narrow ribs the porosity is even more decreased as the compression pressure on those parts is increased.

The flow-field plates of laboratory cells are usually made of graphite. Graphite has good electrical and heat conduction properties, is mechanically rigid, and chemically stable. The graphite plates used in fuel cells are usually impregnated in order to make the structure impermeable of reactant gases. The main disadvantage of graphite is the high cost of bulk material. In addition, graphite is a difficult material to machine. Thus, graphite does not seem suitable for low-cost serial production.

Other materials studied for flow-field plates are different kinds of steel and other metallic structures, see e.g. [33-38], and carbon-based composites, see e.g. [39-43]. Metallic structures are usually cheap and mechanically rigid, which enables thin structures. However, metals are prone to corrosion and usually have high contact resistances. These properties can be improved with surface treatments such as noble metal coating. Composite materials are light and the molding of them is inexpensive. However, good mechanical strength and impermeability of reactants together with high electrical and thermal conductivities are difficult to achieve.

A flow-field plate operates usually as a combined structure in a fuel cell stack. One plate may have the anode and cathode gas channels on the opposite sides of the plate. Such structure is called a bipolar plate. If the fuel cell has active cooling, e.g. air or water circulation, the cooling channels are usually integrated into the bipolar plates.

2.2.5 Other Components

A fuel cell needs also other components besides those mentioned above. These include gaskets, endplates, gas manifolds, and some kind of a clamping mechanism such as bolts. Gaskets have to be chemically stable and impermeable for gases in order to avoid direct contact of reactants and to prevent the leakage of fuel out of the cell. In addition, usually the gaskets have to be electrical insulators as from a practical point of view the membrane is made smaller than the plates of the cell. Gaskets are typically made of different kinds of rubbers and Teflon®-based materials. End plates are used to pile up the fuel cell components and to offer proper mechanical support for the cell. The components of a fuel

cell are usually clamped together with bolts, and thus endplates have to bear high mechanical stress.

A Fuel cell system may have several auxiliary devices controlling the operation of the cell. These include compressors, pumps, mass flow controllers, gas humidifying units, temperature regulators, a gas purification system, and different kinds of diagnostics. These components are used to actively improve the performance or to ensure the operation of the cell. However, the total volume of the system is increased with auxiliary devices, and usually all of the components consume also power. The question, whether the auxiliary devices are beneficial in terms of power density and efficiency of the system, depends very much on the application. For small-scale applications it may be desirable to use passive methods as much as possible to control the operation.

2.3 Principles of Operation

2.3.1 Theoretical Cell Voltage

A theoretical reversible reaction voltage is defined as the available electric work divided by the charge transferred in the reaction process. It can be shown from the fundamentals of thermodynamics that the reversible voltage, E_{rev}, of a PEMFC is

$$E_{\text{rev}} = -\frac{\Delta H - T\Delta S}{zF} = \frac{-\Delta G}{zF} \tag{4}$$

where T is the temperature, z the number of electrons transferred in one reaction, F the Faraday constant, and ΔH, ΔS, and ΔG the change in enthalpy, entropy, and the Gibbs free energy in reaction (3). The Gibbs free energy is a function of temperature and pressure, and its value is calculated as the change from a reference state ΔG^0:

$$\Delta G(T, p) = \Delta G^0(T) + RT \ln\left(\frac{\prod_{prod} a_{\text{i}}^{\lambda_{\text{i}}}}{\prod_{react} a_{\text{i}}^{\lambda_{\text{i}}}}\right) \tag{5}$$

where p is the pressure, R the gas constant, a_{i} the activity of species i, and λ_{i} the stoichiometric factor of species i. Abbreviations *prod* and *react* refer to the products and reactants, respectively. Thus, the reversible voltage of a PEMFC is

$$E_{\text{rev}} = \frac{-\Delta G^0(T)}{zF} - \frac{RT}{zF} \ln\left(\frac{a_{\text{H}_2\text{O}}}{a_{\text{H}_2} a_{\text{O}_2}^{1/2}}\right) \tag{6}$$

The activities are functions of temperature, pressure, and compositions of the species present in half-cell reactions. Thus, with pure reactants the reversible cell voltage is a function of temperature and pressure. Assuming that product water is formed in liquid state ($a \approx 1$), the reversible potential of a PEMFC using pure hydrogen and oxygen is approximately 1.23 V in STP conditions. The effect of temperature, relative humidity of inlet gas, and the cathode stoichiometry on the reversible cell voltage was recently studied by Noponen [44].

2.3.2 Real Cell Voltage

The actual cell voltage is always lower than the theoretical reversible voltage due to different loss mechanisms. Already the open-circuit potential, i.e. cell voltage when no current is drawn from the cell, is significantly lower than the theoretical one. The decrease is caused by mixed potentials, which are due to possible impurities present e.g. in the electrodes or in the fuel gas, and gaseous hydrogen diffusing through the membrane to the cathode. The latter phenomenon is notable especially when thin membranes are used, which is very often the case with small-scale fuel cells in order to decrease the need of external humidification. The practical open-circuit potential of a PEMFC is typically in the range of 0.9 – 1.1 V.

When current is drawn from the cell, different loss mechanisms, called overpotentials, start to decrease the cell voltage further. Different types of overpotentials are activation overpotential arising from sluggish reaction kinetics, ohmic losses arising from electronic and ionic bulk and interface resistances of materials, and mass diffusion overpotential arising from mass transfer limitations.

A typical current-voltage behavior, i.e. polarization curve, of a PEMFC is illustrated in Figure 2. Three different regions, where different overpotentials are the main factor affecting the shape of the curve, can be distinguished from the curve. It should be noted that the boundaries of different regions are only qualitative, and it can not be said where one region stops and another begins.

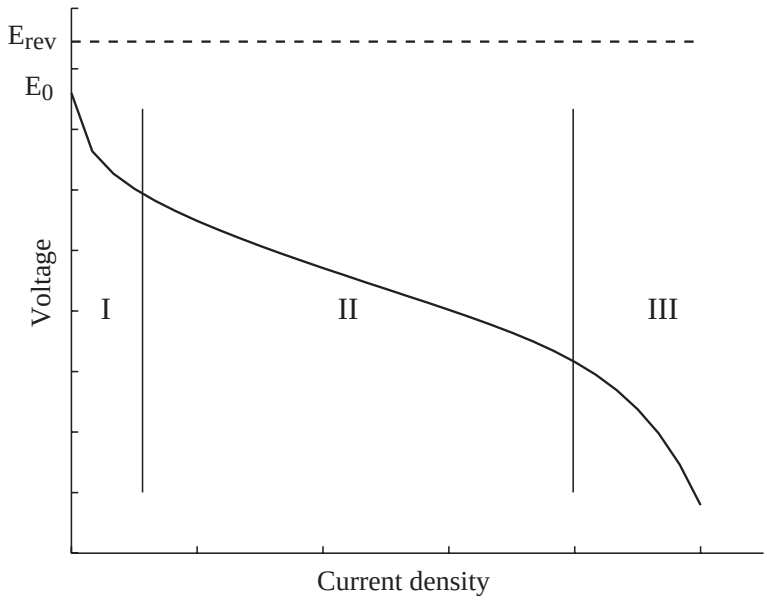

Figure 2. Schematic polarization curve of a PEMFC. The regions where different overpotentials are the main factor affecting the shape of the curve are separated with vertical lines.

At low current densities (Region I in Figure 2) the activation overpotential is the dominating loss mechanism. The main source of activation overpotential is the sluggish oxygen reduction reaction (ORR) at the cathode electrode. The rate-determining step of the ORR is probably the first electron transfer as the oxygen molecule is adsorbed on the platinum catalyst surface, see e.g. [45]. The rate of hydrogen oxidation reaction is orders of magnitude higher than the ORR, and thus if pure hydrogen is used as fuel, the anode side activation overpotential is insignificant loss mechanism in a PEMFC. The activation overpotential caused by the ORR gives the characteristic logarithmic shape of the polarization curve in Region I. Activation overpotential is usually approximated with the Tafel equation

$$\eta_{\text{act}} = a + b\ln(i) \tag{7}$$

where η is the overpotential, subscript *act* refers to activation, a and b are the Tafel constants, and i is the current density. Even though the activation overpotential is typically the highest loss mechanism also at higher current densities, it does not virtually affect the shape of the polarization curve after Region I because of its logarithmic nature.

In the middle part of the current density range (Region II in Figure 2) the major loss mechanism affecting the shape of the polarization curve is the ohmic losses. These arise from the electronic and ionic bulk resistances of the materials, and electronic contact resistances at the component interfaces. The main source of ohmic losses is usually the

proton conducting membrane, but also the contact resistances can have a significant effect on the cell performance as can be seen e.g. from the results of Publication V. The polarization curve is virtually linear in Region II. This is due to the fact that the ohmic losses are directly proportional to the current density (Ohm's law). There may be some deviation from linearity if the conductivity of the membrane is changed e.g. because of a change in humidity.

The shape of the polarization curve at high current densities (Region III in Figure 2) is dominated by the mass diffusion overpotential. This arises from the mass transport limitations, i.e. the decrease in the availability of reactant in the electrode. The cathode is the main source of mass diffusion overpotential because the diffusion of oxygen is significantly slower than the one of hydrogen, and thus the main task in the minimization of mass diffusion overpotential is to maximize oxygen concentration in the electrode. Oxygen concentration in the electrode can be low due to three different reasons listed below.

- Diffusion media can have too low permeability of oxygen resulting in overall reduction of concentration.
- Oxygen concentration can vary between different parts of active area due to fuel cell reactions and non-optimal flow conditions.
- Excess product water, especially if in liquid state, can reduce the porosity of gas diffusion layer and cover parts the catalyst surfaces resulting in spatially heterogeneous oxygen concentration.

The magnitude of pure mass diffusion overpotential can be approximated with the help of Equation (6). At constant pressure the activity of gaseous species can be approximated as its concentration. Thus the overpotential caused by reduced oxygen concentration on the electrode surface is

$$\eta_{\text{diff}} = \frac{RT}{zF} \ln\left(\frac{c_{\text{O}_2}}{c^0_{\text{O}_2}}\right) \tag{8}$$

where η_{diff} is the diffusion overpotential, and c and c^0 are the surface and bulk concentrations of oxygen, respectively.

Even though the approximations for the activation and diffusion overpotentials, such as Equations (7) and (8), may be applicable in some situations, they are actually coupled. Assuming that the electrode is formed of agglomerate structures of carbon-supported platinum catalyst and Nafion® polymer, the area-specific current density of the cathode electrode can be written [46, 47]

$$i = Ai_0 \frac{c_{O_2}}{c_{O_2}^0}(1-\varepsilon_{pol})(1-\varepsilon_{act})(1-s)Eff_{nuc}\exp\left(\frac{-\alpha_c F}{RT}\eta\right) \quad (9)$$

where Ai_0 is the area-specific exchange current density, ε_{pol} the volume fraction of polymer in agglomerate nucleus, ε_{act} the volume fraction of pores in the active layer, Eff_{nuc} the effectiveness factor of an agglomerate (accounts for the diffusion limitations in the agglomerate), and α_c the symmetry factor for ORR. Possible liquid water saturation is also taken into account in Equation (9) as was suggested by Birgersson et al. [48]. The saturation, s, is the volume fraction of the pores occupied by liquid water. The cathode overpotential in Equation (9) is defined as

$$\eta = \phi_e - \phi_p - E_0 \quad (10)$$

where ϕ_e and ϕ_p are the electronic and protonic potentials on cathode electrode, respectively, and E_0 is the open-circuit potential. It is worth noting that the overpotential is defined negative here.

A simplified schematic of 1-D potential profile through a PEMFC is illustrated in Figure 3. An approximation for the real cell voltage, i.e. the voltage between the anode and cathode current collectors (typically the flow-field plates), is obtained when total ohmic losses are subtracted from the cathode and membrane potentials assuming that the anode activation and mass diffusion overpotentials are insignificant. Thus, the cell voltage, E, is

$$E = E_0 - iR + \eta \quad (11)$$

where R is the total area-specific cell resistance including all electronic and ionic bulk and contact resistances.

The real current density range of PEMFCs varies significantly depending on the cell structure and operating conditions. With cells having forced convection and pure oxygen in the cathode, even 2 A cm^{-2} can be achieved with reasonable operating voltage in proper operating conditions. With free-breathing PEMFCs operating without external heating or humidification in ambient conditions, a current density of 100 mA cm^{-2} may be difficult to achieve with reasonable operating voltage.

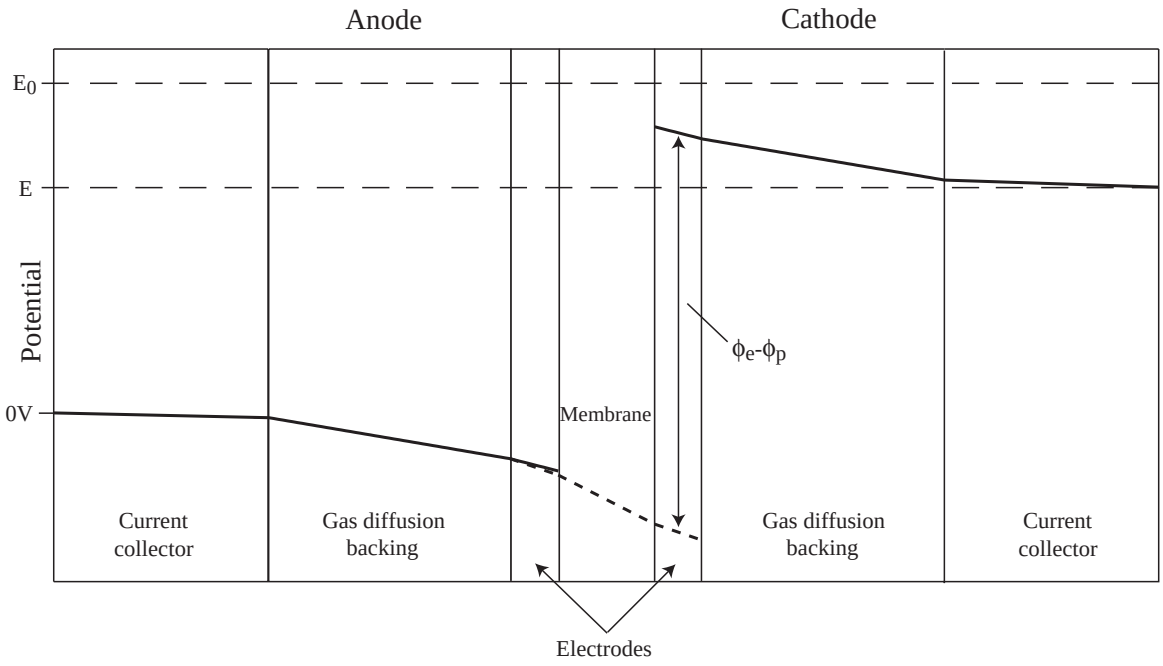

Figure 3. Schematic 1-D potential profile through a PEMFC. Electronic potential is illustrated with solid and protonic potential with dashed line. Real cell voltage is the difference between electronic potentials of anode and cathode current collectors.

2.3.3 Efficiency

This sub-chapter concentrates only on the electric efficiency of a PEMFC. It is not practicable in small-scale application to utilize the heat produced by the fuel cell reactions and different loss mechanisms. Thus, in order to maximize the fuel utilization and simultaneously increase the usage time of application or decrease storage volume of fuel, electric efficiency should be as high as reasonably possible.

The reversible cell efficiency, η_{rev}, is the maximum energy available for electric work divided by the chemical energy of the fuel, i.e.

$$\eta_{\text{rev}} = \frac{-\Delta G}{-\Delta H} \tag{12}$$

The cell voltage is decreased due to different loss mechanisms already at open-circuit potential and especially when current is drawn from the cell, as was described in the previous subchapter. The voltage efficiency is the ratio between the real cell voltage and the theoretical maximum voltage defined in Equation (4):

$$\eta_{\text{V}} = \frac{E}{E_{\text{rev}}} = \frac{zFE}{-\Delta G} \tag{13}$$

Current efficiency is the ratio between the current taken from the cell and theoretical maximum current that a certain hydrogen flow would produce:

$$\eta_{\mathrm{I}} = \frac{I}{I_{\mathrm{theor}}} = \frac{I}{zF\dot{n}_{\mathrm{H_2}}} \tag{14}$$

where I is the current, subscript *theor* refers to theoretical, and $\dot{n}_{\mathrm{H_2}}$ is the molar flow rate of hydrogen. Current efficiency is reduced by fuel losses, such as possible cell leakages and hydrogen penetration from anode to cathode through the membrane. Fuel losses are usually very small compared to flow rates. The main factor typically decreasing the current efficiency is an over-stoichiometric flow of fuel, i.e. more hydrogen is fed through the cell than would be theoretically needed. This decrease can be avoided e.g. by circulating excess hydrogen or operating the fuel cell in dead-end mode as was done e.g. in [49]. Hence, it may possible to achieve current efficiencies close to unity.

The total electric efficiency of a PEMFC, η_{FC}, is achieved by multiplying the efficiency components in Equations (12) – (14):

$$\eta_{\mathrm{FC}} = \eta_{\mathrm{rev}}\eta_{\mathrm{V}}\eta_{\mathrm{I}} = \frac{EI}{-\Delta H\dot{n}_{\mathrm{H_2}}} \tag{15}$$

which is the electric power taken from the cell divided by the chemical power of the hydrogen flow.

If the fuel cell is used to power also auxiliary devices needed by the fuel cell system, the electric power available for the application is decreased. If auxiliary devices are run by an external power source such as battery, the power input of the system is increased. Thus, the total system efficiency, η_{sys}, is

$$\eta_{\mathrm{sys}} = \frac{EI - P_{\mathrm{aux,FC}}}{-\Delta H\dot{n}_{\mathrm{H_2}} + P_{\mathrm{aux,ext}}} \tag{16}$$

where $P_{\mathrm{aux,FC}}$ and $P_{\mathrm{aux,ext}}$ are the power demand of auxiliary devices provided by the fuel cell and an external power source, respectively.

2.4 Local Phenomena

Local performance between different parts of the cell can vary highly. This can be due to e.g. spatial variation in oxygen concentration on the cathode electrode, heterogeneous hydration of the membrane, partial flooding of the electrode, and possible temperature gradients throughout the cell. In order to be able to optimize the cell performance, it is

important to be able to measure or predict these local phenomena and their causes, and to understand the interconnections between them. For example, the saturation pressure of water vapor is an exponential function of temperature, and thus temperature distribution may have significant effect on the mass transfer via flooding if the cell is operated near two-phase conditions.

One important local phenomenon is the current distribution of the fuel cell. Current distribution measurement gives a detailed insight into the problem areas of the cell, because the overpotentials have to be larger in the areas where less current is produced. Current distributions can be measured by direct measuring of different segments, see e.g. [50-56] or with Hall sensors [57, 58]. In segmented cell approach, the current collector is divided into parallel conductive segments which are electrically isolated from each other. A current distribution measurement system for a free-breathing PEMFC built at the laboratory of Advanced Energy Systems at HUT is used in Publications I-IV. An image of the segmented flow-field plate used is presented in Figure 4.

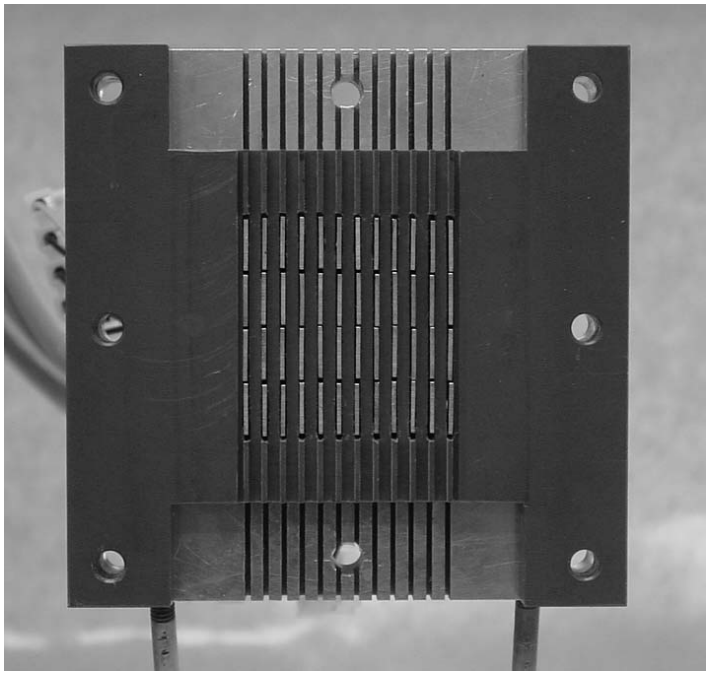

Figure 4. Image of the segmented flow-field plate used in the measurements of Publications I-IV.

The flow-field plate consists of 13 parallel flow channels and the current collector is divided into 48 isolated fragments, which can measure current distribution from a fuel cell that has an active area of 25 cm^2. The current collector pins form the ribs of the channels, which implies that the measurement system measures only ‘global’ current

distribution. With segmented cell approach it is extremely difficult, if not impossible, to measure local current distribution in the horizontal plane of gas diffusion backing surface, i.e. the differences between the regions below channel and below rib. Some additional information would be gained if the current collector pins forming one rib were divided into several isolated micro-structures in horizontal direction, but still the current distribution under the channel would remain unknown. Thus it is important to develop models that can predict also local current distributions. Modeling approaches predicting local concentration and current distributions are presented e.g. in [48, 59-67].

Besides current distribution measurements, several other local phenomena mapping methods have been presented. These include e.g. measuring of water distribution and temperature distribution. Vie and Kjelstrup [68] used thin thermocouples to measure the temperature profile trough the cell and concluded that temperature difference of over 5 °C may exist between electrode and flow-field plate. Ihonen et al. [29] made similar conclusions by measuring the thermal properties of gas diffusion backings ex-situ and non-isothermal models presented by Birgersson et al. [48] and Nguyen et al. [67] implied temperature differences even up to 7 °C. Hakenjos et al. [56] used infrared camera to measure the temperature profile on the surface of a gas diffusion backing. They noticed a temperature difference of several degrees between the middle and edge parts of the cell active area. Similar observations were also made in Publication VII. Thus, significant temperature differences can exist in an operating PEMFC.

Water management is an important task in a PEMFC because the membrane needs to be hydrated in order to have proper protonic conductivity, and possible flooding of the electrodes and gas diffusion backings increase mass transfer limitations significantly. Neutron radiography imaging technique has been used e.g. to measure water gradient profiles inside Nafion® membranes by Bellows et al. [69] and to predict liquid water profile along the cathode gas channels by Geiger et al. [70]. Mench et al. [71] measured the water concentration profile in the gas channel by gas chromatography, and Hakenjos et al. [56] used visual observation of flooding profile in the gas channel with a transparent backside of the flow-field plate. Visual observation of liquid water saturation was also made in Publication VII. PEMFC models taking the effect of liquid water saturation and two-phase mass transfer into account have been presented e.g. in [48, 62, 63, 72, 73].

3 Free-Breathing PEMFC with Vertical Cathode Channels

In a traditional free-breathing PEMFC, the cathode channels are open to ambient air from both ends. In addition to this thesis, this kind of a cell design has been studied e.g. in [49, 74-77]. Term free-breathing refers to the natural convection by which the oxygen needed by the cell reaction is transferred into the cell. Natural convection of air in the cathode channels is driven by buoyancy, which is caused by temperature and gas composition gradients. Temperature gradient is caused by the heat generated in cell reactions and losses and with possible external heating of the cell. Changes in gas composition are caused by the cathode reactions which consume oxygen and produce water.

A free-breathing PEMFC with vertical cathode channels was studied in Publications I-IV. Current distribution measurement system that was shortly described in the previous chapter was used in all measurements. Besides introducing the measurement system, the effect of temperature difference between the cell and ambient air was studied in Publication I by externally heating the cell into a desired temperature. In addition, the error caused by the non-segmented gas diffusion backing was shortly analyzed. The effect of ambient conditions on the cell performance without external heating of the cell was studied in Publication II by placing the fuel cell into a climate chamber in which temperature and relative humidity of air could be controlled. A method for estimating the magnitude of different overpotential distributions with the aid of a highly over-stoichiometric air pulse was introduced in Publication III. A model for cathode channel and gas diffusion backing was developed in Publication IV in order to achieve estimates for molar fractions and flow velocities inside the cell. Measured current distributions were used as a boundary condition for the model.

It was concluded in Publication I that the current distribution of a free-breathing PEMFC can be measured with reasonable accuracy by segmenting the cathode side flow-field plate. A simulation was performed by which it was shown that the non-segmented gas diffusion backing slightly smoothes the measured distribution but should not distort the results significantly. In addition, Noponen et al. [78] reported that the segmentation of a gas diffusion backing easily results in a membrane failure at high current densities because there is no proper mechanical support for the MEA at the segmented edges resulting in overheating due to decreased thermal conductivity.

The cell temperature levels used in Publication I were ambient, 45 °C, 60 °C, and 75 °C. It should be noted that in Publication I the ambient cell temperature refers to a measurement in which the cell was not externally heated. The cell temperature in this measurement was 31 – 34 °C, and thus it was a few degrees higher than the temperature of the surrounding air. In higher temperatures the cell was heated with two external

heating elements placed into holes drilled into opposite sides of the anode side endplate. The cell temperature was measured by a thermocouple placed into a hole drilled into the upper part of the anode side flow-field plate.

The polarization curves from the measurements of Publication I are redrawn in Figure 5. The performance of the cell is improved as the cell temperature is increased from ambient to 60 °C. Further temperature increase led to significant performance loss. The increase in cell temperature enhances airflow in the cathode channels, which brings more oxygen to the electrode and improves removal of excess water. This effect can be seen in Figure 6, where the current distributions with the average current density of 100 mA cm^{-2} at an ambient cell temperature and 60 °C are illustrated. At the lower temperature the bottom of the cell is producing significantly more current than the upper parts of the cell, implying that the convection was not strong enough to ensure homogeneous concentration profile along the channel. At the higher temperature the current distribution is rather uniform due to a higher airflow rate.

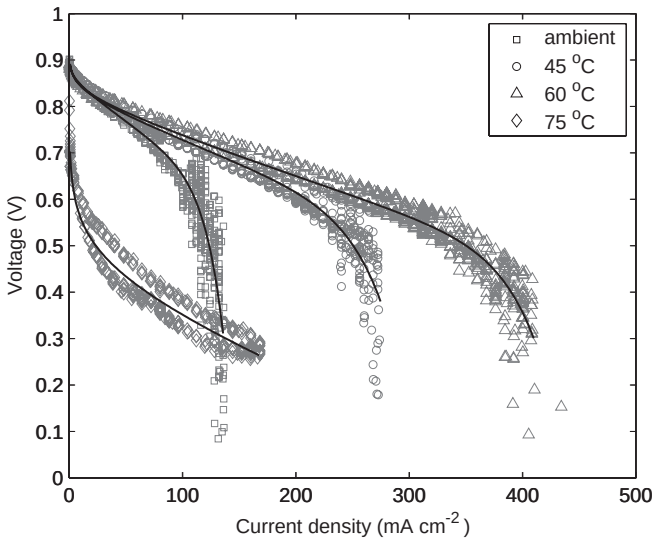

Figure 5. Polarization curves from measurement with different cell temperatures. Legend ‘ambient’ refers to the case where the cell was not externally heated.

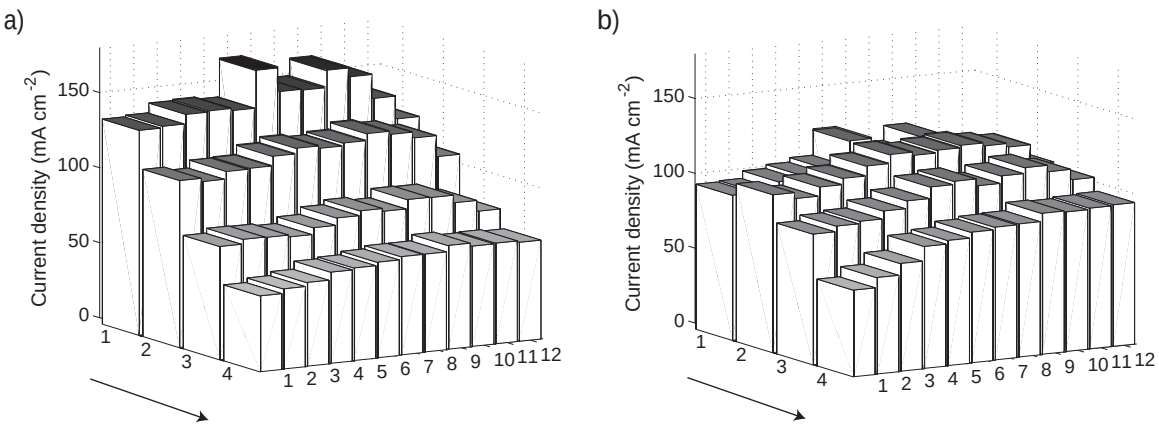

Figure 6. Current distribution at the average current density of 100 mA cm^{-2}; a) ambient cell temperature, b) cell temperature of 60 °C. Flow direction is indicated with an arrow.

It was concluded that the optimum operation temperature for this kind of fuel cell design without external humidification is somewhere near 60 °C. Poor cell performance at a cell temperature of 75 °C was concluded to be due to drying of the proton conducting phases. However, even a temperature of 60 °C may be impracticable for a free-breathing cell. Heating of the cell requires power and possible insulation increases the size of the cell. Both of these situations are unfavorable for fuel cells that are most probably applicable only in small-scale applications.

If the cell is not externally heated, the ambient temperature should have an effect on the operation of a free-breathing PEMFC. The airflow, and thus also the oxygen supply and the water removal, in the channels are proportional to the temperature difference between the cell and the surrounding air. This airflow transfers part of the generated heat from the cell to the surroundings. The rest is transferred by thermal radiation and convection from the surfaces of the cell. The radiative heat transfer is proportional to the difference between absolute cell temperature to fourth power and absolute ambient temperature to fourth power, see e.g. [79]. Thus, at a higher ambient temperature a smaller temperature difference is needed to provide the same radiative heat transfer rate. Depending on the ratio of different heat transfer mechanisms, there may be significant deviation in temperature difference between the cell and surroundings at varying ambient conditions resulting in non-similar airflow rates.

The effect of varying ambient conditions without external heating of the cell was studied in Publication II. The polarization curves measured at ambient temperatures of 10 °C and 40 °C with varying relative humidity are presented in Figure 7. The effect of humidity in the lower temperature is insignificant whereas at higher temperature the mass diffusion overpotential starts to affect the shape of the curve at notably smaller current densities when the humidity is increased. The saturation pressure of water vapor is an exponential

function of temperature and thus there is a huge difference in absolute humidity between these temperatures. However, even at 40 °C the difference in oxygen concentration between totally dry and saturated air is only approximately 7%. The 5% difference mentioned in Publication II is between the lowest and highest humidity levels used in the measurements, not between totally dry and saturated air.

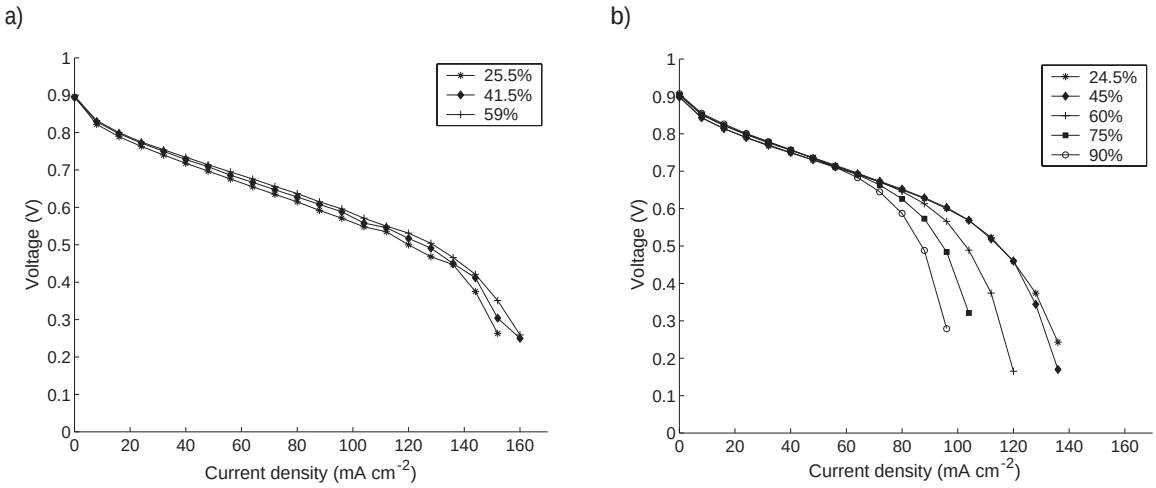

Figure 7. a) Polarization curves from measurement with ambient temperature of 10 °C; b) polarization curves from measurement with ambient temperature of 40 °C. The legends in the figure refer to the relative humidity.

The main difference in cell conditions between different ambient temperatures was that at higher temperatures the cell did not heat up as much. Thus, there was a smaller temperature gradient between the cell and air, implying that radiation is a significant heat transfer mechanism for this kind of a cell. As a result, the airflow in the cathode channels was weaker at higher ambient temperatures. The cell temperature remained quite constant between different humidity levels at constant ambient temperature, implying that also the airflow in the channels should have been rather similar in these measurements. However, there is still significant difference in performance and current distributions as is illustrated in Figure 8.

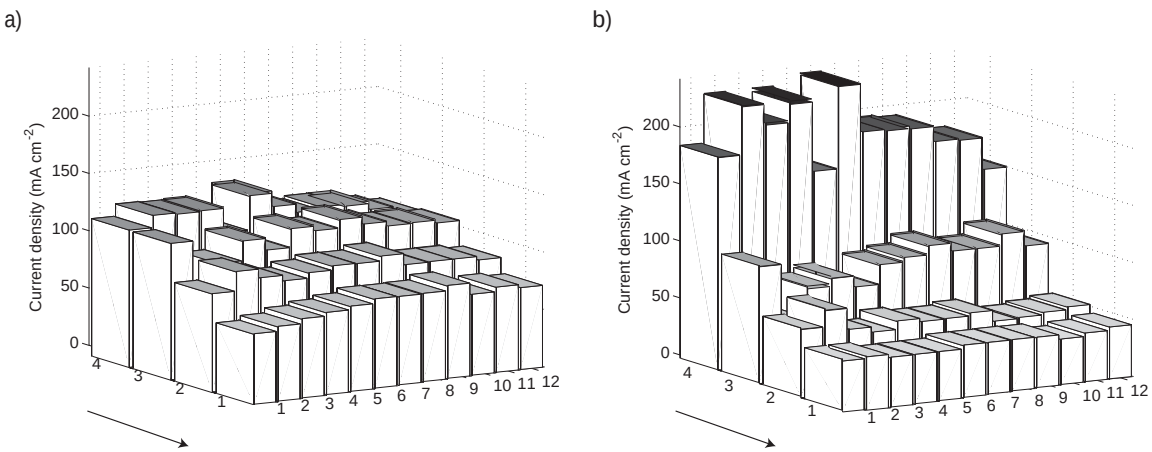

Figure 8. Current distributions at ambient temperature of 40 °C; a) relative humidity 24.5%, b) relative humidity 90%. The bottom part of the cell is at row 4. Flow direction is indicated with an arrow.

At the high humidity level (Figure 8b) almost all of the current is produced in the lower parts of the cell whereas at the lower humidity level (Figure 8a) the current distribution is much more homogeneous. Because the airflow rate should have been fairly similar and the difference in oxygen concentration in air was quite small, it was concluded that the reason for performance loss was flooding. Flooding started at the upper parts of the cell and increased towards lower parts as the humidity was increased. It was concluded that in order to improve the performance of this type of a cell, the temperature difference between the cell and ambient air should be as high as reasonably possible.

In publication III, a method to estimate the magnitude and distribution of mass diffusion overpotential in a free-breathing PEMFC from the current distribution measurements was introduced. The method was based on the measurement of the voltage difference between operation under natural and forced convection. Forced convection was accomplished by feeding a highly over-stoichiometric air pulse to the cathode channels. It was assumed that the air pulse was strong enough to create a uniform oxygen concentration distribution inside the cell and thus to eliminate the differences in mass diffusion overpotential.

Examples of calculated mass diffusion overpotential distributions are illustrated in Figure 9. At the lower current density level the absolute difference between mass diffusion overpotential at the top and bottom parts of the cell is rather small, whereas at the higher current density level the difference is almost an order of magnitude larger. The larger mass diffusion overpotential in the edge parts of the cell seen in Figure 9 is probably due to the fact that the edge channels were narrower than other channels. In addition, the temperature in the middle parts of the cell is most probably higher than at the edge parts, and thus may also affect the shape of the mass diffusion overpotential distribution.

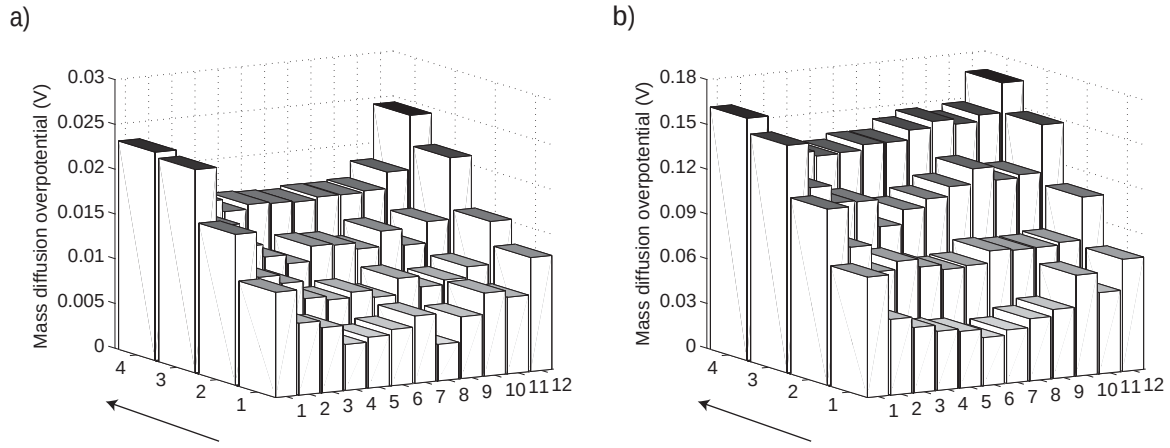

Figure 9. Calculated mass diffusion overpotential distributions; a) average current density of 60 mA cm^{-2}, b) average current density of 180 mA cm^{-2}. The bottom part of the cell is at row 1. Flow direction is indicated with an arrow.

A model for a similar cell structure as was used in current distribution measurements was developed in Publication IV. The model took cathode channel and gas diffusion backing into account and used measured current distributions as boundary condition for reactions. The model was steady-state, isothermal, and in one phase. The transport of species was modeled with Navier-Stokes equation including a buoyancy term in the channel, and with Maxwell-Stefan diffusion in the gas diffusion backing. The purpose of this study was to predict the concentration profiles and airflow in the cathode of a free-breathing PEMFC, and thus also gain more insight into the limiting processes affecting the cell performance. The modeled cases were cell temperatures of 40 and 60 °C with different current density levels. An example of oxygen molar fraction profiles in the gas channel and gas diffusion backing predicted by the model is illustrated in Figure 10.

The modeling results verified the conclusion made in previous publications that the better performance at a higher cell temperature is mainly due to higher air flow rate caused by temperature-driven convection. According to the model, the flow velocity at the higher cell temperature is over 50% larger leading to a more homogeneous oxygen concentration profile and to more effective water removal. At the lower cell temperature the partial pressure of water vapor exceeds the saturation pressure, implying that the cell is at least partially flooded.

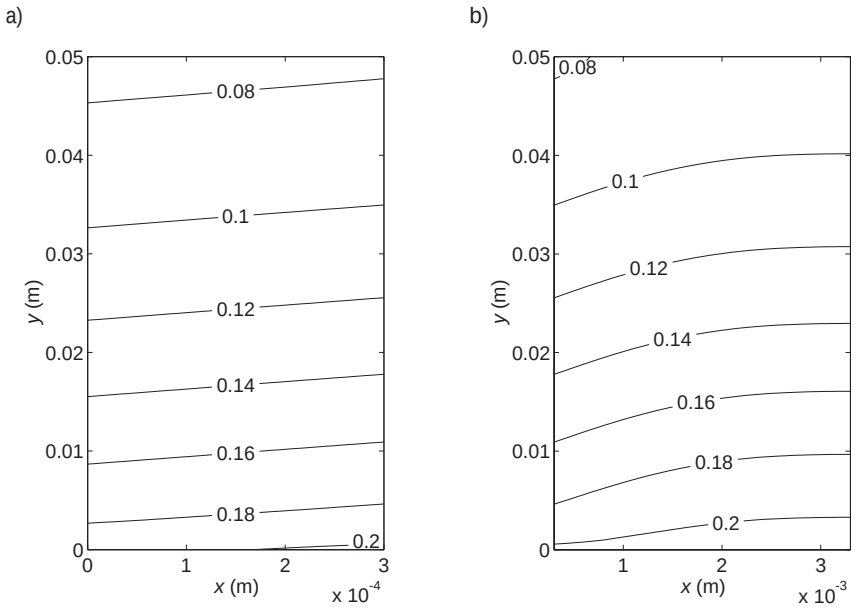

Figure 10. Molar fractions of oxygen at cell temperature of 60 °C and average current density of 300 mA cm^{-2}; a) gas diffusion backing, b) gas channel.

In addition, a measurement series with the cathode channels in horizontal direction was conducted in Publication IV. In horizontal direction the thermal gradient does not create buoyancy-driven convection, and thus the main driving force is diffusion. Polarization curves from these measurements and vertically averaged current distributions (i.e. distribution in horizontal direction) with different average current density levels at the cell temperature of 40 °C are illustrated in Figure 11. The spatial resolution in the direction of the channels is poor, but qualitative conclusions can still be made from the distribution. The middle parts of the cell produce significantly less current than the edge parts, showing that the diffusion is not strong enough to transfer oxygen to the whole active area of the cell. Thus, it can be concluded that the mass transfer rate caused by diffusion is significantly lower than that caused by convection. The average current density did not exceed the value of 56 mA cm^{-2} in these measurements. The slightly poorer performance of the other edge of the cell seen in Figure 11b (line 1) is most probably due to drying out of the proton conducting phases caused by dry hydrogen fed in from that part of the cell.

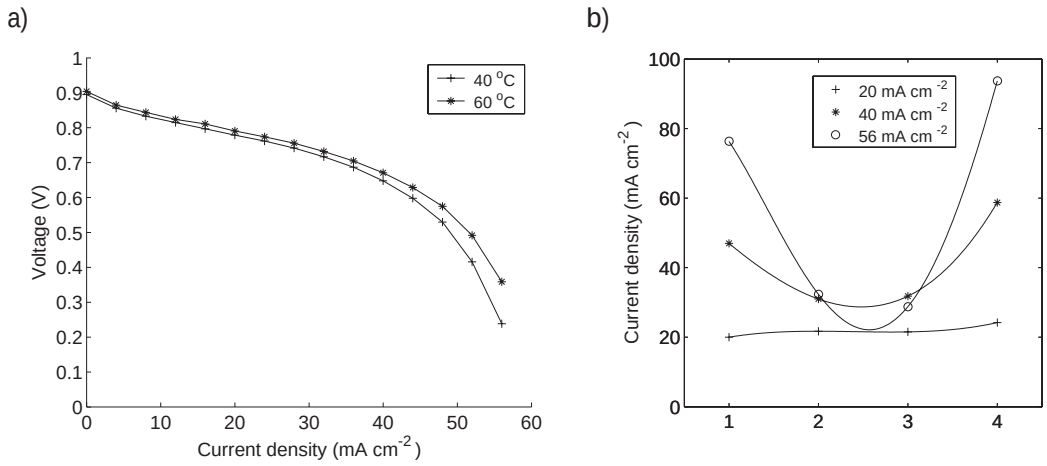

Figure 11. a) Polarization curves from the measurement with the channels in horizontal direction, b) vertically averaged current distributions with different average current density levels at cell temperature of 40 °C. A polynomial fit is made to the averaged distribution data in order to make the shape of the distribution clearer.

In publication I it was said that in an ambient cell temperature the main driving force was diffusion. This is only partially true, as this would have been the case if there were no temperature difference between the cell and air. However, there was a temperature difference of a few degrees also in this measurement and thus there were also convection occurring in the channels. Results of Publication II imply that even with a temperature difference of a few degrees convection has a significant effect on cell performance, and if the diffusion was the main driving force, similar behavior in the central parts of the cell should have been seen as in Figure 11b.

The oxygen concentration profile calculated from the results of Publication III and the corresponding profile predicted by the model introduced in Publication IV were recently compared by Noponen [44]. It was noted that the concentration profiles predicted by different methods differ radically from each other. The flow pulse method gave a significantly smaller oxygen concentration than the model. The model does not take liquid water into account and it was shown in Publication IV that the saturation pressure of water vapor is exceeded. Thus, there should be liquid water present inside the cell, implying that the model predicts too high an oxygen concentration on the electrode surface. On the other hand, the flow pulse method may not necessarily provide totally homogeneous oxygen concentration profile on the electrode, and strong air pulse may also dry out the proton conducting phases leading into differences in resistance. Thus, the flow pulse method may also give misleading results.

According to the results presented in Publications I-IV and here, it seems that the main limitation with this kind of a cell design is the mass transfer in the cathode channels. In

order to enhance the air flow and thus to improve mass transfer, there should be high temperature gradient between the cell and ambient air. Higher cell temperature would also decrease flooding because the saturation pressure of water is an exponential function of temperature. High temperature gradient could be accomplished e.g. by external heating or with insulation of the cell. Neither of these is favorable in terms of system power density, because external heating consumes power and insulation increases the size of the system. One possible solution could be e.g. using flow-field plate materials that have low thermal conductivity. However, if the current is collected through the flow-field plate structure, the material should have high electric conductivity, which is not typical for materials having low thermal conductivity.

Mass transfer could also be improved by decreasing the flow resistance of the channels. The flow resistance is inversely proportional to the cross-sectional area, and thus wider and/or deeper channels would enhance the flow. However, the cross-sectional area of the channels cannot be increased without limitations as was discussed in Subchapter 2.2.4.

It was concluded that when the cell is not externally heated, the major phenomenon limiting the performance is flooding. Flooding starts from the upper part of the channels as the upward flowing air gets gradually more humidified and eventually exceeds the saturation point. Thus, the flooding could be decreased if the channels were shorter. In some measurements the flooding was so severe that there were liquid water droplets blocking some of the channels. Some kind of hydrophobic coating of the channels could be beneficial in order to improve water removal from the channels.

As an overall conclusion, it seems that this kind of a cell design is not optimal for applications in which the orientation of the cell can vary, such as most portable electronics. However, with an optimized cell, the situation can be totally different, especially with applications that are in certain orientation most of the usage time. In addition, the effect of orientation could most probably be decreased with shorter channels. Hence, with careful optimization this kind of a cell design may have potential in small-scale applications.

4 Titanium Sinter as Gas Diffusion Backing

It was concluded in the previous chapter that the main limitation of a free-breathing PEMFC is the cathode side mass transfer. With a free-breathing PEMFC it would be beneficial, in terms of mass transfer, to increase the cross-sectional area of the channels because of decreased flow resistance. If the channels were made wider, a rigid gas diffusion backing material would be needed in order to provide enough mechanical support as was discussed in Subchapter 2.2.4. Hence, rigid materials may be beneficial compared to carbon papers as a gas diffusion backing. Such a rigid material, sintered titanium, was studied in Publication V.

Sintered materials have also the advantageous property that the gas channels may be formed directly into the sinter during the sintering process [30]. This would simplify the cell structure as one component could operate as an integrated gas diffusion backing / flow-field plate. This could also decrease the total cost of the fuel cell as the separate manufacturing process of gas channels would be eliminated.

It was noticed in the experiments that a Ti sinter has a high contact resistance with the MEA. Different kinds of coatings were applied on the sinter in order to reduce this contact resistance. In addition to the evaporated platinum and carbon coatings presented in Publication V, a few carbon black based solutions were sprayed on the sinter, but even after heat treatment they did not attach to the surface of sinter well enough and they were left out of consideration.

Some of the polarization and resistance curves from the measurements presented in Publication V are illustrated in Figure 12. Traditional carbon paper gas diffusion backing was used as a reference in order to be able to evaluate the performance of Ti sinter. With proper coating, the decrease in contact resistance was significant. The total resistance of the cell compared to the measurement with carbon paper was over six times higher with plain Ti sinter and approximately three times higher with platinum coated Ti sinter. The platinum coating also seemed to improve the mass transfer on the cathode side. The platinum coating probably increased the hydrophobic properties of the Ti sinter, and thus enhanced water removal from the cell.

It could be assumed that the platinum coating also contributes to the catalysis of the reactions due to direct contact with the electrode surface. However, the reactions need a three phase boundary in order to occur as explained in Subsection 2.2.2 and a protonic conductor is present only in the electrode. Hence, the increase in the active catalyst surface area should be negligible, and the catalytic effect of the coating is therefore most likely also insignificant. This can also be concluded from the results of Publication V.

Comparing the IR-compensated polarization curves it can be noticed that there is very little difference between carbon paper and coated Ti sinters at low current densities. This implies that there was no significant difference in the activation overpotential suggesting that the platinum coating did not contribute to the catalysis of the reactions.

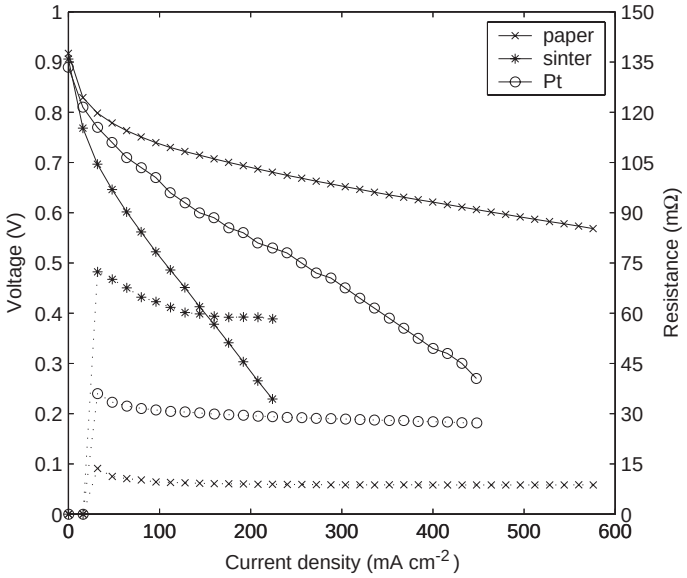

Figure 12. Polarization (solid line) and resistance (dashed line) curves from the measurements with Ti sinter. ‘paper’ refers to the reference measurement with carbon paper, ‘sinter’ to the measurement with plain Ti sinter, and ‘Pt’ to measurement with Ti sinter having 5 nm platinum coating.

The results show that Ti sinter operates somewhat poorer as a gas diffusion backing than traditional carbon paper. However, the advantages offered by the mechanical rigidity of sinter may outweigh this performance loss in some situations, such as with a free-breathing PEMFC having wider vertical channels. This can be especially the case if the sinter forms one integrated gas diffusion backing / flow-field plate structure.

5 Planar Free-Breathing PEMFC

As a result of characterization of a free-breathing PEMFC with vertical cathode channels it was concluded that the cathode side mass transfer is the major factor limiting performance. In addition to the wider channels suggested, a totally different kind of a cathode design could be an interesting alternative in order to improve the performance. A so-called planar free-breathing cell design is studied in Publications VI and VII. The structure of a planar free-breathing PEMFC is illustrated in Figure 13.

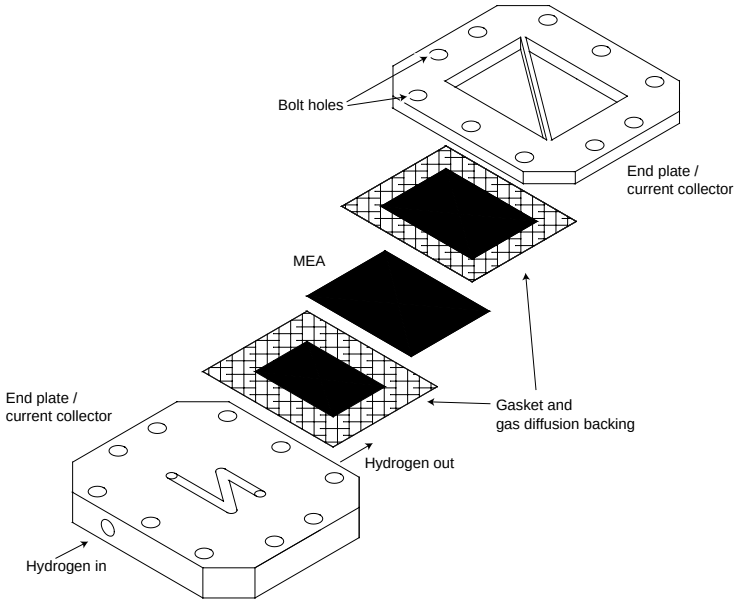

Figure 13. Structure of a planar free-breathing PEMFC. The cathode gas diffusion backing is directly open to ambient air.

In a planar cell, the cathode gas diffusion backing is directly in contact with ambient air, and hence there is no need for cathode side flow-field plate at all. The cell structure is such that it enables thin large-area cells. Even though the thickness of the planar cell studied in this thesis was not optimized in any way, it is possible to reduce the thickness down to a few millimeters, see e.g. [80, 81]. Hahn et al. [82] demonstrated a planar cell aimed for very small applications that was only 200 μm thick.

The concept of a planar cell design was evaluated in Publication VI. In these measurements, a mechanically rigid cathode gas diffusion backing was used in order to enable large unsupported areas for oxygen diffusion. Polarization curves with two different thick carbon sheet gas diffusion backings, namely #18802 and #19802, are illustrated in Figure 14. The performance difference between materials is due to materials properties. #18802 was more porous and had a higher resistance. Polarization curve from measurement with #18802 in vertical cell orientation is also illustrated in Figure 14. This

measurement was performed in order to see the effect of cell orientation. There is no apparent difference between polarization curves in different orientation, which implies that the convection occurring on the surface of the cell was adequate in order not to limit the performance.

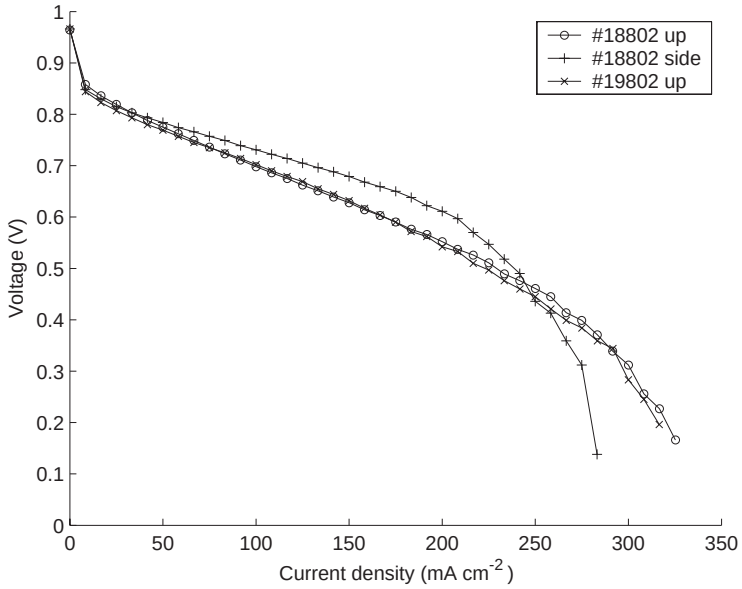

Figure 14. Polarization curves with two different mechanically rigid carbon sheet gas diffusion backings. Notation ‘up’ refers to horizontal cell orientation (cathode side upwards) and ‘side’ to vertical cell orientation.

Current transient measurements were also conducted in Publication VI. The results showed that with a small base load (50 mA cm^{-2}) the cell was capable of producing momentarily high current densities. The response for current transients was decreased with a higher base load. This implies that if the fuel cell is designed for a small base load then the cell itself is capable of managing some short-term power peaks. However, if the maximum power point is chosen as the operating point, then virtually all power peaks have to be managed with capacitors or batteries.

The effect of cathode structure of a planar free-breathing PEMFC was studied in Publication VII. Three different gas diffusion backings and three different current collector plates were used on the cathode. The gas diffusion backings were rigid carbon sheet used in Publication VI, Ti sinter used in Publication V, and a thin compressible carbon paper. The difference between the current collector plates was the width of the openings between the current collecting ribs.

The structure of a cathode current collector plate has a similar effect on losses occurring in a planar cell as the channel-rib ratio discussed in Subchapter 2.2.4. If there are large openings between current collecting ribs, total resistance is increased as the current

produced in the middle of the openings has a longer way to reach the current collector. However, the effective area for oxygen diffusion is simultaneously increased and thus mass diffusion overpotential is decreased.

With rigid and thicker gas diffusion backings, this effect should be smaller because the oxygen has a longer way to diffuse, enabling a more homogeneous oxygen concentration profile on the electrode. However, with thicker gas diffusion backings, the mass diffusion overpotential is increased because the absolute value of oxygen concentration on the electrode is smaller. On the other hand, a thin and compressible gas diffusion backing is more compressed under the ribs, causing loss of porosity which increases mass diffusion limitations. With fewer ribs supporting a compressible gas diffusion backing, poor contact between MEA and GDB may exist in the middle of the openings, increasing the contact resistance of those parts.

Results from the measurements with different gas diffusion backings showed that with thicker gas diffusion backings, the effect of current collector plate structure was not as significant as with a thin and compressible gas diffusion backing. With thick carbon sheet there was only small difference in performance and with somewhat thinner Ti sinter the effect was already noticeable especially with largest openings. With large openings the resistance was slightly increased and mass transfer was improved as was assumed.

The polarization curves with a thin and compressible gas diffusion backing are illustrated in Figure 15a. The effect of current collector plate is clear. With the largest openings the cell performance is decreased drastically as resistance is increased. With smaller openings high power densities for a free-breathing PEMFC were achieved with a maximum of approx. 360 mW cm^{-2}. In the middle of the current density range liquid water saturation on the top of the gas diffusion backing was noticed, implying water removal limitations. With higher current densities the water droplets disappeared as the cell heated up.

The effect of cell orientation with carbon paper gas diffusion backing was studied with current collector plate having 2 mm wide openings. Polarization curve with cell in vertical orientation is also illustrated in Figure 15a. The cell performed somewhat better in vertical direction than in horizontal direction, implying that with a thin gas diffusion backing the convective mass transfer becomes a limiting factor for cell performance and that the convection was enhanced in this direction.

Correlations for averaged convective heat and mass transfer coefficients can be found from literature. The Nusselt numbers for free-convection occurring on isothermal horizontal and vertical flat plates based on correlations found from [79] are calculated in Appendix A. The values with different characteristic lengths were slightly higher for vertical plate. The average heat flux is proportional to the Nusselt number and because of

the analogy between heat and mass transfer coefficients the result implies that the convective mass transfer rate is higher in vertical direction. However, the real situation is far more complicated than an isothermal flat plate through which there is no mass transfer. In addition, the value of the Rayleigh number from which the Nusselt number for horizontal plate with smaller characteristic length was calculated was on the lower applicability limit of the correlation. Thus, these figures should be taken only as qualitative approximations.

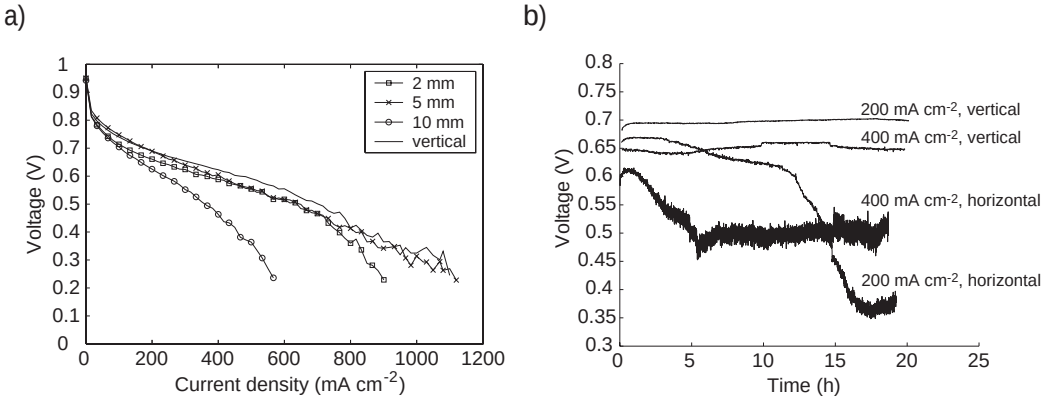

Figure 15. Results from the measurements with carbon paper gas diffusion backing: a) Polarization curves with different current collector plates. Size notations refer to the width of the current collector openings and 'vertical' to the measurement with cell in vertical orientation. b) Long-term measurements with current collector plate having 2 mm openings. The average current density and cell orientation is given next to the corresponding curve.

There were long-term measurements performed with a carbon paper gas diffusion backing in Publication VII because liquid water condensation was observed during the polarization measurements. Also these measurements in different cell orientations implied convective mass transfer limitations. The results from the long-term measurements are illustrated in Figure 15b. The convective mass transfer limitations are apparent in horizontal cell direction. With an average current density of 400 mA cm^{-2} the surface of the gas diffusion backing was partly blocked by liquid water, and with 200 mA cm^{-2} most of the surface was flooded. The effect of liquid water saturation can be seen in Figure 15b as the voltage decreases significantly due to increased mass diffusion overpotential.

The mass transfer limitations caused by liquid water saturation in long-term measurements should not be critical in real small-scale applications as they are not necessarily even observed. For example, most portable electronics are idle (operate on a very small load) most of the time, and high power demand for several hours in a row seems implausible.

On the basis of the results achieved in Publications VI and VII, it seems that a planar cell design is a potential power source for small-scale applications. With planar cell design very thin free-breathing PEMFCs are possible. With a banded cell structure, proposed e.g. by Heinzel et al. for forced-convection cell [83], it is possible to make free-breathing planar cell stacks. A schematic structure of a possible planar cell stack is illustrated in Figure 16. With planar cell stack the voltage and power demands of an application are easily fulfilled by increasing the active area and number of unit cells. A thin large-area planar cell stack could be integrated, e.g., into the cover of a laptop computer.

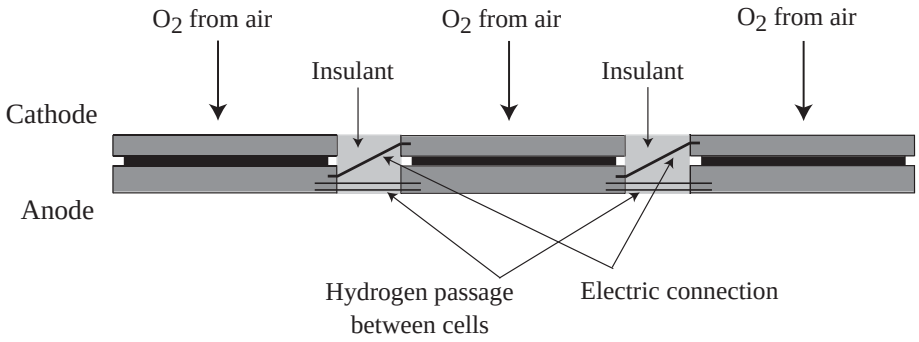

Figure 16. Schematic illustration of a free-breathing planar stack using banded cell structure.

6 Summary and Concluding Remarks

This thesis concentrates on free-breathing polymer electrolyte membrane fuel cells (PEMFCs). The term free-breathing refers to the use of passive methods for supplying the oxygen needed by the cell reactions directly from ambient air. Two different kinds of free-breathing cell designs were studied and a potential new type of a gas diffusion backing material was introduced in this thesis. The aim of this thesis was to identify the performance limitations caused by the use of passive air supply in small-scale PEMFCs and to find solutions for these limitations.

The first cell design is a traditional free-breathing PEMFC in which vertical cathode channels are open to ambient air from both ends. The air for the reactions is brought to cell by natural convection occurring in the channels. The other cell design is a planar free-breathing PEMFC. In planar cell design, the cathode side of the cell is directly open to ambient air and there are no cathode gas channels at all. This kind of a cell design enables large free area for cathode side mass transfer. The material introduced was titanium sinter, and it was used as a mechanically rigid gas diffusion backing.

The free-breathing PEMFC with vertical cathode channels was studied with current distribution measurement system introduced in Publication I. The effect of the cell temperature and ambient conditions were studied in Publications I and II. Different overpotential distributions were studied with the flow pulse method in Publication III. A model developed for cathode gas channel and gas diffusion backing was introduced in Publication IV. The purpose of the model was to predict the molar fractions and flow velocities in the cathode.

According to the results presented in Publications I-IV and in Chapter 3, it is concluded that the main limitation with this kind of a cell design is the mass transfer in the cathode channels. In order to enhance the air flow and thus to improve mass transfer, there should be a high temperature gradient between the cell and ambient air. Higher cell temperature would also decrease flooding because the saturation pressure of water is an exponential function of temperature. The mass transfer could also be improved by decreasing the flow resistance of the channels. This could be accomplished e.g. by increasing the cross-sectional area of the channels. However, both of these methods to improve the mass transfer have their own limitations.

The need for a supporting structure is decreased with a rigid gas diffusion backing material, which would enable e.g. wider cathode channels. Titanium sinter was studied as a potential gas diffusion backing material in Publication V. The main problem with Ti sinter was high contact resistance with the MEA. Even though the contact resistance

could be significantly reduced with a platinum coating, the performance was still weaker than with traditional carbon paper gas diffusion backings. However, the results showed that Ti sinter may have potential in some applications. This would be especially the case if the gas channels were directly formed to the structure during the sintering process and Ti sinter was used as a combined gas diffusion backing / flow-field plate.

Another solution for the improvement of cathode side mass transfer limitations can be a so-called planar free-breathing cell design. The planar free-breathing cell was introduced in Publication VI and the effect of cathode structure on its performance was studied in Publication VII. The results showed that this kind of a cell design might be advantageous for free-breathing PEMFCs. Different cathode setups in Publication VII included three different gas diffusion backing materials and three different current collector plate structures. With thick and rigid gas diffusion backings, the effect of a current collector plate structure was significantly smaller than with a thin and compressible carbon paper gas diffusion backing. Very high power densities for a free-breathing PEMFC were achieved with certain cathode structures.

It was concluded from the results of Publication VII that with a thin gas diffusion backing, the convection occurring on the surface of planar cell becomes a limiting factor. The water removal in some cases was not adequate and significant liquid water saturation was observed. Thus the cell structure needs to be further optimized in order to ensure the long-term operation also with high power densities. However, high power densities for several hours in a row are not typical for small-scale applications, and thus it is not necessarily a critical issue.

As an outcome of this thesis, the performance limiting factors caused by the use of passive air supply in the PEMFC are better understood and possible solutions for these limitations are introduced and discussed. As a result, a free-breathing PEMFC with a very high area-specific power density was achieved.

The general conclusion of this thesis is that the free-breathing PEMFCs, especially planar cell design, have potential to replace batteries in small-scale applications. For example, assuming a portable computer with an average power consumption of 20 W and a planar cell producing stable 200 mW cm^{-2}, there would easily be enough area to integrate the cell into the laptop cover. The mass of a typical laptop battery is approximately 400 g. If this mass was replaced with a metal hydride hydrogen storage having a storage capacity of 3 mass-%, there would be approximately 400 Wh of energy available. Assuming that the total electric efficiency of a planar cell system was approximately 0.45, the continuous usage time with one hydrogen fill would be approximately 9 hours which is significantly more than the typical operating time of a laptop computer run with a battery.

Even though the results are promising, there are still issues to be solved before the cells can be brought to large-scale commercial market. The cell structure and materials should be further optimized in a way that the cathode side mass transfer is improved increasing the power density and especially ensuring stable cell operation for applications where long-term high power operation is needed. In addition, efficient storage of hydrogen, especially in terms of system volumetric and/or gravimetric power density, is a major problem with small-scale PEMFC applications. One solution for hydrogen storage problems is the use of direct methanol fuel cells (DMFCs) because liquid methanol is significantly easier to store than hydrogen. However, DMFCs typically have lower power density than PEMFCs. Thus, it depends on the applications and fuel refill infrastructure whether the performance loss is outweighed by the easiness of fuel storage.

References

[1] The U.S. Energy Information Administration, Annual Energy Review 2002, http://www.eia.doe.gov/emeu/aer/, cited 8.4.2004

[2] U. Bossel, *The Birth of the Fuel Cell 1835-1845*, European Fuel Cell Forum, Oberrohrdorf, Switzerland, 2000

[3] A.J. Appleby, F.R. Foulkes, *Fuel Cell Handbook*, van Nostrand Reinhold, New York, USA, 1989

[4] M.L. Perry, T.F. Fuller, J. Electrochem. Soc. 149 (2002) 59-67

[5] M. Eikerling, A.A. Kornyshev, U. Stimming, J. Phys. Chem. B 101 (1997) 10807-10820

[6] S.J. Paddison, J. New Mat. Electrochem. Systems 4 (2001) 197-207

[7] A.Z. Weber, J. Newman, J. Electrochem. Soc. 150 (2003) 1008-1015

[8] T.A. Zawodzinski, C. Derouin, S. Radzinski, R.J. Sherman, V.T. Smith, T.E. Springer, S. Gottesfeld, J. Electrochem. Soc. 160 (1993) 1041-1047

[9] T.A. Zawodzinski, J. Davey, J. Valerio, S. Gottesfeld, Electrochim. Acta 40 (1995) 297-302

[10] M. Ise, K.D. Kreuer, J. Maier, Solid State Ionics 125 (1999) 213-223

[11] F. Meier, G. Eigenberger, Electrochim. Acta 49 (2004) 1731-1742

[12] K. Dannenberg, *Characterization and Modelling of the PEMFC*, Doctoral Dissertation, Royal Institute of Technology, Stockholm, Sweden, 2002

[13] O. Himanen, *Hydrogen-Hydrogen Cell as Research Tool for Polymer Electrolyte Membrane Fuel Cells*, Master's thesis, Helsinki University of Technology, 2003

[14] H. Nakajima, S. Nomura, T. Sugimoto, S. Nishikawa, I. Honma, J. Electrochem. Soc. 149 (2002) 953-959

[15] K.T. Adjemian, S. Srinivasan, J. Benziger, A.B. Bocarsly, J. Power Sources 109 (2002) 356-364

[16] P. Costamagna, C. Yang, A.B. Bocarsly, S. Srinivasan, Electrochim. Acta 47 (2002) 1023-1033

[17] L. Qingfeng, H.A. Hjuler, N.J. Bjerrum, J. Appl. Electrochem. 31 (2001) 773-779

[18] M. Rikukawa, K. Sanui, Progress Polym. Sci. 25 (2000) 1463-1502

[19] L. Giorgi, A. Pozio, C. Bracchini, R. Giorgi, S. Turtù, J. Appl. Electrochem. 31 (2001) 325-334

[20] C. Roth, M. Goetz, H. Fuess, J. Appl. Electrochem. 31 (2001) 793-798

[21] F.A. de Bruijn, D.C. Papageorgopoulos, E.F. Sitters, G.J.M. Janssen, J. Power Sources 110 (2002) 117-124

[22] H.A. Gasteiger, J.E. Panels, S.G. Yan, J. Power Sources 127 (2004) 162-171

[23] M. Mikkola, *Experimental Studies on Polymer Electrolyte Membrane Fuel Cell Stacks*, Master's thesis, Helsinki University of Technology, 2001

[24] L. Giorgi, E. Antolini, A. Pozio, E. Passalacqua, Electrochim. Acta 43 (1998) 3675-3680

[25] C.S. Kong, D.-Y. Kim, H.-K. Lee, Y.-G. Shul, T.-H. Lee, J. Power Sources 108 (202) 185-191

[26] Z. Qi, A. Kaufman, J. Power Sources 109 (2002) 38-46

[27] J.Chen, T. Matsuura, M. Hori, J. Power Sources 131 (2004) 155-161

[28] M. Prasanna, H.Y. Ha, E.A. Cho, S.-A. Hong, I.-H. Oh, J. Power Sources 131 (2004)147-154

[29] J. Ihonen, M. Mikkola, G. Lindbergh, J. Electrochem. Soc. 151 (2004) 1152-1161

[30] P.J. Mitchell, International Patent WO 98/52241 (1998)

[31] C. Zawodzinski, M.S. Wilson, in: *Proceedings of the second international symposium on proton conducting membrane fuel cells*, Electrochem. Soc. Proceedings Vol. 98-27 (1999) 446-456

[32] S. Gamburzev, A.J. Appleby, J. Power Sources 107 (2002) 5-12

[33] D.P. Davies, P.L. Adcock, M. Turpin, S.J. Rowen, J. Power Sources 86 (2000) 237-242

[34] R.C. Makkus, A.H.H. Janssen, F.A. de Bruijn, R.K.A.M. Mallant, J. Power Sources 86 (2000) 274-282

[35] J. Wind, R. Späh, W. Kaiser, G. Böhm, J. Power Sources 105 (2002) 256-260

[36] N. Cunningham, D. Guay, J.P. Dodelet, Y. Meng, A.R. Hlil, A.S. Hay, J. Eletrochem. Soc. 149 (2002) 905-911

[37] H. Wang, M.A. Sweikart, J.A. Turner, J. Power Sources 115 (2003) 243-251

[38] H. Wang, J.A. Turner, J. Power Sources 128 (2004) 193-200

[39] J. Scholta, B. Rohland, V. Trapp, U. Focken, J. Power Sources 84 (1999) 231-234

[40] T.M. Besmann, J.W. Klett, J.J. Henry Jr., E. Lara-Curzio, J. Electrochem. Soc. 147 (2000) 4083-4086

[41] D. Busick, M. Wilson, Materials Research Society Symposium Proceedings (New Materials for Batteries and Fuel Cells) 575 (2002) 247-251

[42] E.A. Cho, U.-S. Jeon, H.Y. Ha, S.-A. Hong, I.-H. Oh, J. Power Sources 125 (2004) 178-182

[43] A. Heinzel, F. Mahlendorf, O. Niemzig, C. Kreuz, J. Power Sources 131 (2004) 35-40

[44] M. Noponen, *Current Distribution Measurements and Modeling of Mass Transfer in Polymer Electrolyte Fuel Cells*, Doctoral Dissertation, Helsinki University of Technology, Espoo, Finland, 2004

[45] M.D. Maciá, J.M. Campiña, E. Herrero, J.M. Feliu, J. Electroanal. Chem. 564 (2004) 141-150

[46] F. Jaouen, G. Lindbergh, G. Sundholm, J. Electrochem. Soc. 149 (2002) 437-447

[47] J. Ihonen, F. Jaouen, G. Lindbergh, A. Lundblad, G. Sundholm, J. Electrochem. Soc. 149 (2002) 448-454

[48] E. Birgersson, M. Noponen, M. Vynnycky, *Heat Transfer Phenomena in Polymer Electrolyte Fuel Cells*, submitted to J. Electrochem. Soc. 2004

[49] T. Mennola, M. Noponen, T. Kallio, M. Mikkola, T. Hottinen, J. Appl. Electrochem. 34 (2004) 31-36

[50] S.J.C. Cleghorn, C.R. Derouin, M.S. Wilson, S. Gottesfeld, J. Appl. Electrochem. 28 (1998) 663-672

[51] J. Stumper, S.A. Campbell, D.P.Wilkinson, M.C. Johnson, M. Davis, Electrochim. Acta 43 (1998) 3773-3783

[52] D.J.L. Brett, S. Atkins, N.P. Brandon, V. Vesovic, N. Vasileiadis, A.R. Kucernak, Electrochem. Commun. 3 (2001) 628-632

[53] N. Rajalakshmi, M. Raja, K.S. Dhathathreyan, J. Power Sources 112 (2002) 331-336

[54] G. Bender, M.S. Wilson, T.A. Zawodzinski, J. Power Sources 123 (2003) 163-171

[55] M.M. Mench, C.Y. Wang, M. Ishikawa, J. Electrochem. Soc. 150 (2003) 1052-1059

[56] A. Hakenjos, H. Muenter, U. Wittstadt, C. Hebling, J. Power Sources 131 (2004) 213-216

[57] Ch. Wieser, A. Helmbold, E. Gülzow, J. Appl. Electrochem. 30 (2000) 803-807

[58] Y.-G. Yoon, W.-Y. Lee, T.-H. Yang, G.-G. Park, C.-S. Kim, J. Power Sources 118 (2003) 193-199

[59] A. Kazim, H.T. Liu, P. Forges, J. Appl. Electrochem. 29 (1999) 1409-1416

[60] A.A. Kulikovsky, J. Divisek, A.A. Kornyshev, J. Electrochem. Soc. 146 (1999) 3981-3991

[61] S. Dutta, S. Shimpalee, J.W. Van Zee, J. Appl. Electrochem. 30 (2000) 135-146

[62] D. Natarajan, T. Van Nguyen, J. Electrochem. Soc. 148 (2001) 1324-1335

[63] T. Berning, D.M. Lu, N. Djilali, J. Power Sources 106 (2002) 284-294

[64] T. Berning, N. Djilali, J. Power Sources 124 (2003) 440-452

[65] J.J. Hwang, C.K. Chen, R.F. Savinell, C.C. Liu, J. Wainright, J. Appl. Electrochem. 34 (2004) 217-224

[66] S. Um, C.Y. Wang, J. Power Sources 125 (2004) 40-51

[67] P.T. Nguyen, T. Berning, N. Djilali, J. Power Sources 130 (2004) 149-157

[68] P.J.S. Vie, S. Kjelstrup, Electrochim. Acta 49 (2004) 1069-1077

[69] R.J. Bellows, M.Y. Lin, M. Arif, A.K. Thompson, D. Jacobson, J. Electrochem. Soc. 146 (1999) 1099-1103

[70] A.B. Geiger, A. Tsukada, E. Lehmann, P. Vontobel, A. Wokaun, G.G. Scherer, Fuel Cells 2 (2002) 92-98

[71] M.M. Mench, Q.L. Dong, C.Y. Wang, J. Power Sources 124 (2003) 90-98

[72] Z. H. Wang, C.Y. Wang, K.S. Chen, J. Power Sources 94 (2001) 40-50

[73] N.P. Siegel, M.W. Ellis, D.J. Nelson, M.R. von Spakovsky, J. Power Sources 128 (2004) 173-184

[74] D. Chu, R. Jiang, J. Power Sources 83 (1999) 128-133

[75] S.O. Morner, S.A. Klein, J. Solar Energy Eng. 123 (2001) 225-231

[76] T. Mennola, M. Mikkola, M. Noponen, T. Hottinen, P. Lund, J. Power Sources 112 (2002) 261-272

[77] P.-W. Li, T. Zhang, Q.-M. Wang, L. Schaefer, M. K. Chyu, J. Power Sources 114 (2003) 63-69

[78] M. Noponen, J. Ihonen, A. Lundblad, G. Lindbergh, J. Appl. Electrochem. 34 (2004) 255-262

[79] F.P. Incropera, D.P. DeWitt, *Fundamentals of Heat and Mass Transfer*, 2nd ed., John Wiley & Sons, Inc., Singapore, 1985

[80] A. Schmitz, M. Tranitz, S. Wagner, R. Hahn, C. Hebling, J. Power Sources 118 (2003) 162-171

[81] A. Schmitz, S. Wagner, R. Hahn, H. Uzun, C. Hebling, J. Power Sources 127 (2004) 197-205

[82] R. Hahn, S. Wagner, A. Schmitz, H. Reichl, J. Power Sources 131 (2004) 73-78

[83] A. Heinzel, C. Hebling, M. Müller, M. Zedda, C. Müller, J. Power Sources 105 (2002) 250-255

Appendix A: Calculation of Correlations for Free-Convection

The correlation of the Nusselt number, *Nu*, for a vertical isothermal flat plate is [79]

$$Nu = 0.68 + \frac{0.670 Ra^{1/4}}{\left[1 + \left(0.492 / Pr\right)^{9/16}\right]^{4/9}}, \qquad 0 < Ra < 10^9 \tag{A.1}$$

where *Ra* is the Rayleigh number and *Pr* the Prandtl number defined as

$$Ra = \frac{g\beta\left(T_S - T_{amb}\right)L^3}{\nu\alpha} \tag{A.2}$$

$$Pr = \frac{\nu}{\alpha} \tag{A.3}$$

where g is the gravitational acceleration, β the volumetric thermal expansion coefficient, T_S the plate temperature, T_{amb} the temperature of ambient air, L the characteristic length, ν the kinematic viscosity, and α the thermal diffusivity. For an ideal gas the volumetric thermal expansion coefficient is inversely proportional to temperature. Here the average temperature between the plate and ambient air is used.

The correlation of the Nusselt number for the upper side of a horizontal heated isothermal flat plate is [79]

$$Nu = 0.54 Ra^{1/4}, \qquad 10^4 \lesssim Ra \lesssim 10^7 \tag{A.4}$$

Values of standard air at 300 K [79] are used in the calculations. The temperatures of ambient air and the plate are assumed to be 20 and 30 °C, respectively, and the characteristic lengths of 0.02 and 0.03 m are used (the edges of the active area). The resulting Nusselt numbers with the characteristic length of 0.02 m are 5.44 for vertical and 5.00 for horizontal plate. With the characteristic length of 0.03 m the corresponding values are 7.14 for vertical and 6.78 for horizontal plate.

The Rayleigh number with the characteristic length of 0.02 m is 7370, which is near the lower applicability limit of Equation (A.4). Thus, the achieved value of Nusselt number for horizontal plate with smaller characteristic length should be used with caution.